1,3-DIPOLAR CYCLOADDITION OF AN ISOXAZOLINE N-OXIDE TO OLEFINS

by

Youn Yuen Shu

B.Sc., National Chung Hsing University, 1978

THESIS SUBMITTED IN PARTIAL FULFILLMENT OF

THE REQUIREMENTS FOR THE DEGREE OF

MASTER OF SCIENCE

in the Department

of

Chemistry

SIMON FRASER UNIVERSITY

July, 1985

APPROVAL

Name: Youn Yuen Shu

Degree: Master of Science

Title of thesis: 1,3-DIPOLAR CYCLOADDITION OF AN ISOXAZOLINE N-OXIDE TO OLEFINS

Examining Committee:

Chairman: Dr. F. W. B. Einstein, Professor

Y. L. Chow, Professor
Senior Supervisor

K. N. Slessor, Professor
Supervisory Committee

M. J. Gresser, Assoc. Professor
Supervisory Committee

B. L. Funt, Professor
Internal Examiner

Date Approved:

PARTIAL COPYRIGHT LICENSE

I hereby grant to Simon Fraser University the right to lend my thesis, project or extended essay (the title of which is shown below) to users of the Simon Fraser University Library, and to make partial or single copies only for such users or in response to a request from the library of any other university, or other educational institution, on its own behalf or for one of its users. I further agree that permission for multiple copying of this work for scholarly purposes may be granted by me or the Dean of Graduate Studies. It is understood that copying or publication of this work for financial gain shall not be allowed without my written permission.

Title of Thesis/Project/Extended Essay

"1,3-Dipolar Cycloaddition of an Isoxaline N-Oxide to Olefins"

Author:

(Signature)

Youn-Yuen Shu

(name)

Oct. 10, 1985

(date)

ABSTRACT

The 1,3-dipolar cycloaddition of 3-methyl-5-phenyl-isoxazoline N-oxide to electron-poor olefins, such as methyl acrylate, acrylonitrile, styrene, dimethyl fumarate, dimethyl maleate, fumaronitrile, vinyl methyl ketone, and maleic anhydride, gave diastereoisomeric cycloadducts of 1-aza-2,8-dioxabicyclo[3.3.0]-octanes. The N-oxide failed to react with bulky trans-stilbene and electron-rich vinyl acetate. The cycloadditions to the mono-substituted olefins gave only one type of regioisomer. Out of four possible approaches of the 1,3-dipole to the olefins, steric effects in the transition state control the reaction pathway leading to one predominant cycloadduct, the top-exo adduct. For the cycloaddition with maleic anhydride, secondary orbital effects dictate the reaction pathway to give the top-endo adduct. The relative configurations of the majority of these diastereoisomers were determined from their NMR spectra and Nuclear Overhauser Effects.

The formation constants of the ground state complex between the N-oxide and olefins were investigated. Both maleic anhydride and fumaronitrile formed ground state complexes and reacted with N-oxide , while dimethyl fumarate and dimethyl maleate failed to give ground state complex but reacted with N-oxide; trans-stilbene showed strong ground state complex formation but

no reaction was observed.

The stereoselectivities of the cycloadditions with maleic anhydride, dimethyl fumarate, and fumaronitrile were improved under high pressure (1.38 or 2.07 KBar). However, high pressure had no effect on the cycloaddition with methyl acrylate.

To my Parents

ACKNOWLEDGEMENT

The author wishes to express his sincere thanks to Dr.Y.L. Chow for his guidance and genuine interest throughout this work. He also wishes to thank Dr. Slessor, Dr. Gresser and Dr. Buono-Core for their helpful discussions and general assistance. The collaboration and friendship of fellow members of Dr.Chow's group are gratefully acknowledged. The author also wishes to thank Dr.K.E. Newman and the technical staff for their valuable assistance, and particularly to M.Tracey.

A special thanks to Marcia Craig for the very helpful revision of the manuscript.

Financial assistance from the Department of Chemistry, Simon Fraser University is also acknowledged.

TABLE OF CONTENTS

LIST OF TABLES

LIST OF FIGURES

CHAPTER 1

INTRODUCTION

The 1,3-dipolar cycloaddition reaction is one of the most useful reactions for the synthesis of hetereocyclic compounds [1,2]. It provides one of the best tools for constructing five-membered rings and has a nearly singular capability of establishing a large number of stereochemical[3] centers in one synthetic step.

The "1,3-dipole" is a species which can be represented by zwitterionic resonance structures. These zwitterions undergo 1,3-cycloadditions to multiple bond systems, referred to as "dipolarophiles"[1,2].

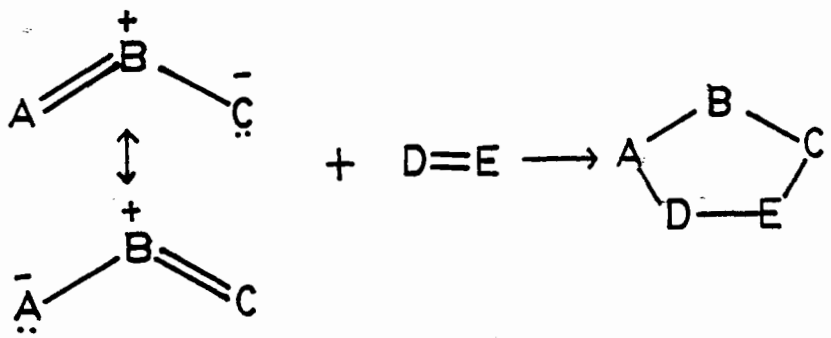

Huisgen proposed a concerted mechanism for the 1,3-dipolar cycloaddition[2,4], and Firestone proposed a two-step diradical mechanism[5,6]. While serious conflicts exist between these two hypotheses, the former has been widely accepted[7,8,9] without critical evaluation. HOMO-LUMO frontier orbital theoretical studies of the mechanism of this reaction have been reported [10,11,12].

The preparation of isoxazolidine derivatives was first reported by Bodforss and then by Kohler in the early 1900's [13]. The cycloadditions of nitrones and olefins have been widely investigated since 1950[14,15]. The fact that nitronic esters undergo 1,3-dipolar cycloaddition to olefins was discovered and developed by Tartakovskii and co-workers in the early 1960's. A wide variety of olefins have been added to methyl dinitromethane nitronate to give cycloadducts in good yields[16].

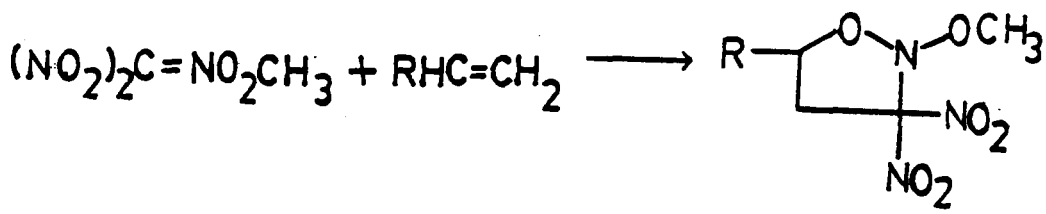

The reaction has been extended to cyclic nitronic esters as in the preparation of 1-aza-2,8-dioxabicyclo[3.3.0]-octanes (isoxazolizidines)(Scheme 1-1) [17]. From

3-nitro-5-R-isoxazoline N-oxide and styrene or ethylene, a mixture of the two isomers (configuration at C-7) is formed (Scheme 1-1 and 3-1). All the cycloadditions were conducted under mild conditions and gave high yields[18].

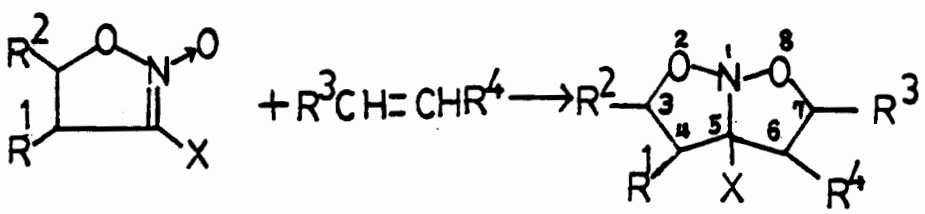

X	R^1	R^2	R^3	R^4
NO_2	H	H	H	H
NO_2	H	Ph	Ph	H
NO_2	H	Me	Me	H
Ph	H	H	H	H
Ph	H	H	Ph	H
COOMe	H	H	Ph	H
COOMe	H	H	COOMe	H

SCHEME 1—1

A number of the cycloproducts synthesized from open-chain nitronic esters and olefins have been reported by Gree et al. They have discussed the physical properties in detail[19,20].

A series of physical and chemical properties of isoxazolizidines has been investigated. Ginzburg et al.[21] found by X-ray analysis that the two five-membered rings of the bicyclic adduct, each in an "envelope" conformation, make a dihedral angle of 115°. The IR absorption of the O-N-O moiety was found in the range 1010-1060 cm^{-1}[22]. The isoxazolizidine ring is UV-transparent, since it is saturated. Therefore, any absorption recorded for isoxazolizidine derivatives is caused by the substituents[23]. When isoxazolidines are treated with an acid, N-O cleavage and other reactions take place (Scheme 1-2). N-Methoxy-3-phenyl-5-methoxycarbonyl-isoxazolidine gives a mixture of isoxazoline and imino alcohol when heated with dry HCl (Scheme 1-3) [24]. In the reduction of N-methoxyisoxazolidines with $LiAlH_4$, loss of methanol takes place to give 2-isoxazolines (Scheme 1-3) [25].

The structures of the bicyclo adducts have been discussed in terms of X-ray diffraction, dipole moments, chemical shifts, and coupling constants. The NMR data together with NOE results reported here give definitive information on their structures.

The investigation of the ground state complex formation indicates that the pathway of the 1,3-dipolar cycloaddition might be controlled by the stereochemistry of the complex. High pressure is expected to influence the stereoselectivities.

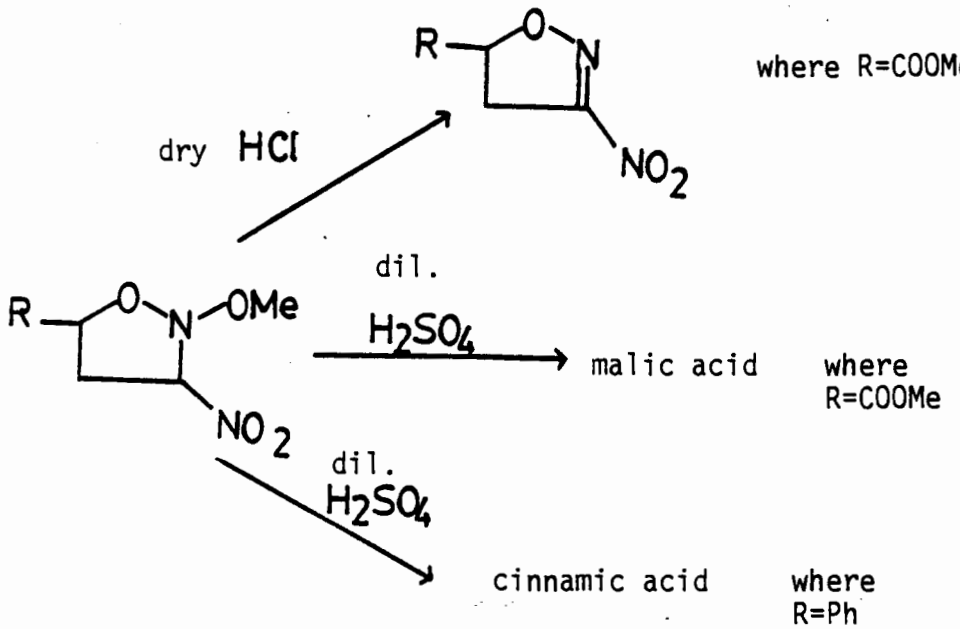

SCHEME 1–2

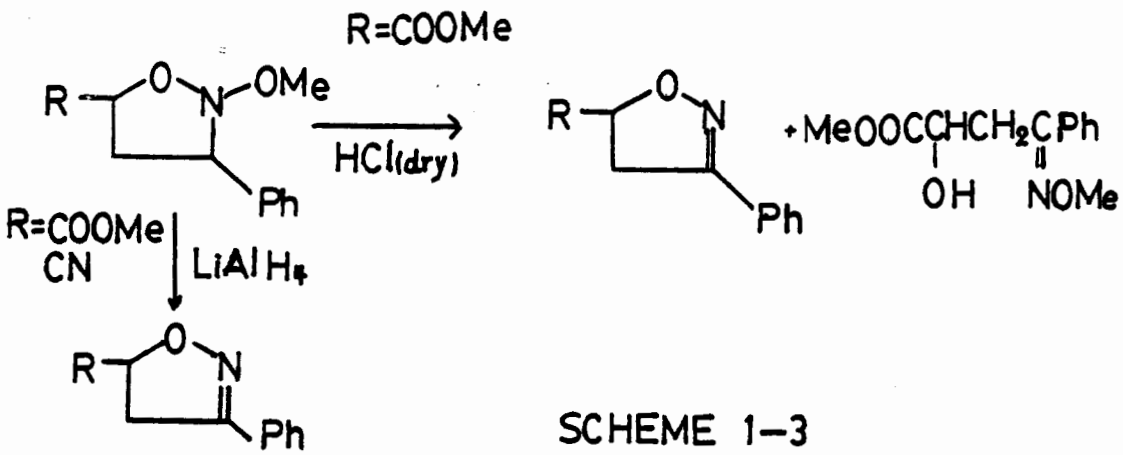

SCHEME 1–3

CHAPTER 2

Results

In view of the ready accessibility of 3-methyl-5-phenyl isoxazoline N-oxide 1, we have investigated the 1,3-dipolar cycloadditions of 1 to olefins to give isoxazolizidine derivatives 2. While such cycloadditions have been investigated by Tartakovskii[26,27] in the early 1960's, their regio- and stereochemistry have not been thoroughly studied. Isoxazolizidine 2 possesses an atomic array of the O-N-O moiety in the molecular frame work; such a group is basically a dialkoxyamine group which may exhibit interesting physical and biological activities, e.g. redox reactions and photo-electron spectroscopy, etc.

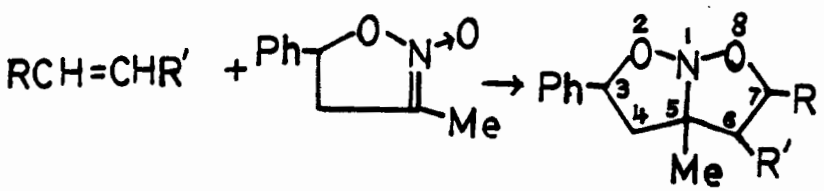

1 2

1. Preparation of 3-methyl-5-phenyl-isoxazoline N-oxide 1

Reaction of 1-phenyl-1-dimethylsulfoniumbromide-2-bromo ethane [28] and nitroethane gave an 85% yield of N-oxide 1. The simple method was developed by Bakker giving high yields of 1.

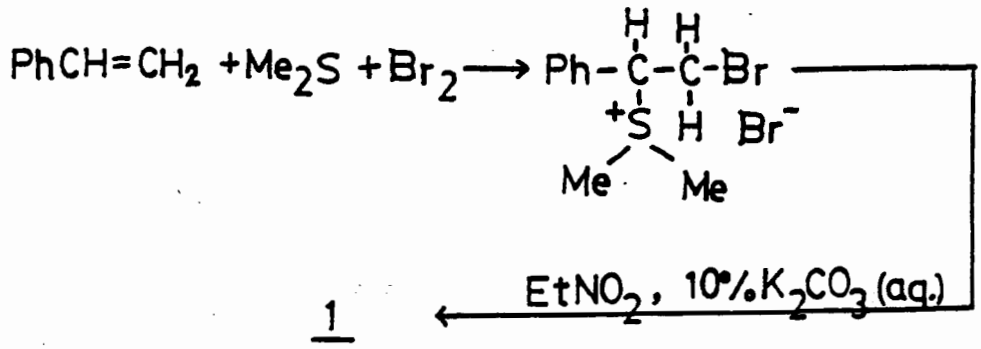

The ^1H NMR spectrum of N-oxide 1 has an ABX pattern of the methylene protons with 16 peaks due to the coupling with methyne proton (dd) and further with methyl protons, and a methyl signal(t). The I. R. spectrum gave a C=N band at 1640 cm^{-1}. The mass spectrum by CI mode(iso-butane) gave an M+1 peak at m/e 178. The mass spectrum by EI mode gave fragments at m/e 41, 51, 77 ($C_6H_5^+$), 91($C_7H_7^+$), 105(base, $C_6H_5CO^+$), 129, 130, and 131. The similar N-oxide 1A[29] which was synthesized by Holy also showed fragments at m/e 51, 77, 105, 130 and 131. The ^{13}C NMR spectrum showed similar chemical shifts and intensities to that for N-oxide 1A.

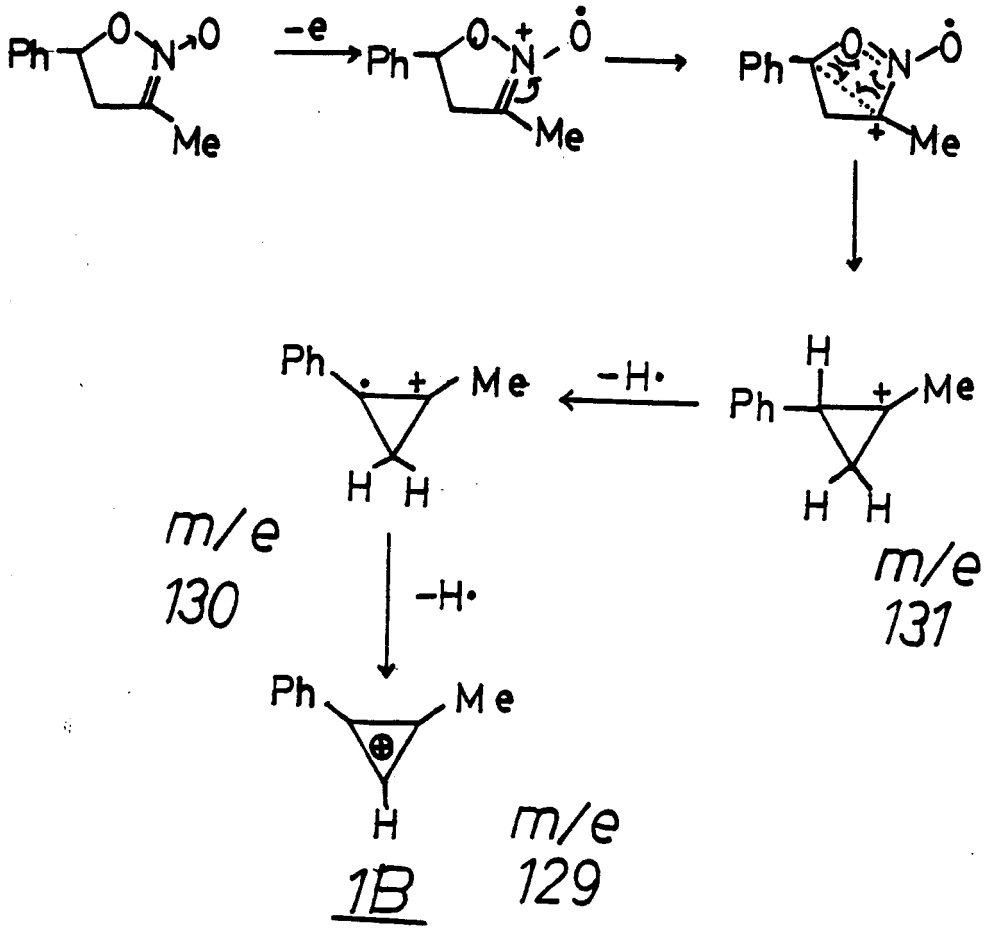
-e
Ph
Me
-H·
m/e
130
m/e
131
m/e
129
1B
1A

2. 1,3-Dipolar Cycloadditions of N-oxide 1 to Olefins

The general method of the cycloadditions were carried out by heating acetonitrile solutions of the two components under nitrogen atmosphere. Analysis based on the methyl peaks of the NMR spectra of the crude thermolysates permitted a determination of the relative amount of the isomeric cycloadducts and the conversion of N-oxide 1. Most cycloadducts could be successfully separated by flash chromatography (acetone-hexane as eluent) or HPLC (isopropanol-hexane as eluent). The Nuclear Overhauser Effect technique[30,31] was applied to determine the structures of cycloadducts. The spectral data of the cycloadducts are listed in Table-9 to Table-15.

The cycloadditions of N-oxide 1 to monosubstituted olefin, such as methylacrylate, styrene and acrylonitrile, can lead to two regioisomers, i.e. head-to-head 3 and head-to-tail 4 adducts. Only the head-to-head type adducts 3 were obtained in these dipolar cycloadditions. The isomer 4 was not observed in all cases from the NMR spectra of crude products and isolated components. The mode of these cycloadditions is similar to the works which have been reported by Tartakovskii and Shimizu [32]. The differentiation of the two isomers is on the basis of observing the chemical shifts of H_a and H_f in the two ABX pattern signals that resemble each other if stereochemistry is not considered. Coupling constants and/or decoupling techniques were used to distinguish these two ABX sets. Both H_a and H_f

possess similar magnetic environments and resonate at low fields with similar chemical shifts. This pattern could not be explained by the structure in 4[32]. This conclusion is confirmed by NOE difference data.

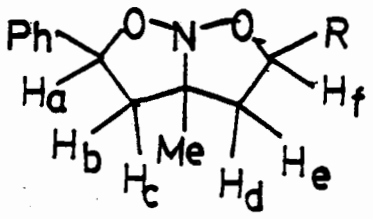

3

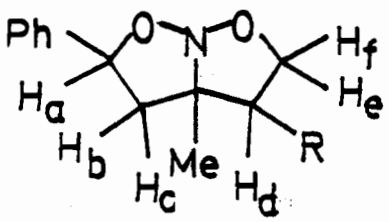

4

R= a.COOMe, b.Ph, c.CN

The stereochemical course of the cycloaddition is depicted in Scheme 2-1 which shows four possible orientations designated as top-exo (TX), bottom-exo (BX), top-endo (TN), and bottom-endo (BN) leading to 5TX, 5BX, 5TN and 5BN, respectively. Owing to steric hindrance of the bottom-endo orientation of the phenyl and R^1 groups, 5BN is regarded to be the least stable product. In cycloaddition to 9 olefins, more than two stereoisomers were observed in the crude products, all but three of which could be isolated in pure or semi-pure states. The conditions of the cycloadditions are summarized in Table-1. The relative yields of the cycloadducts are listed in Table-2.

TABLE-1. REACTION CONDITIONS OF THE CYCLOADDITIONS OF 1 TO OLEFINS.

OLEFINS	REACTION CONDITIONS	CONCENTRATIONS(M) [1]	[OLEFINS]	ADDUCTS
vinyl methyl ketone	144h 45°C	0.16	0.18	two adducts
methyl acrylate	93h 50°C	0.037	0.73	6TX, 6TN, 6BX, 6BN
styrene	120h 50°C	0.04	0.32	7TX, 7TN
acrylo-nitrile	120h 95°C	0.034	0.23	8TX, 8TN, 8BX, 8BN
dimethyl fumarate	432h 85°C	0.023	0.028	9TX, 9TN, 9BN
fumaro-nitrile	168h 82°C	0.057	0.085	10TX, 10TN 10BX, 10BN
maleic anhydride	8h 82°C	0.2	0.14	11BX, 11BN 11TX, 11TN
dimethyl maleate	1008h, 85°C and 1440h 22°C	0.067	0.27	12TX, 12BX
stilbene	216h 95°C	0.025	0.025	none
vinyl acetate	90h 82°C	0.16	0.18	none

SCHEME 2 – 1

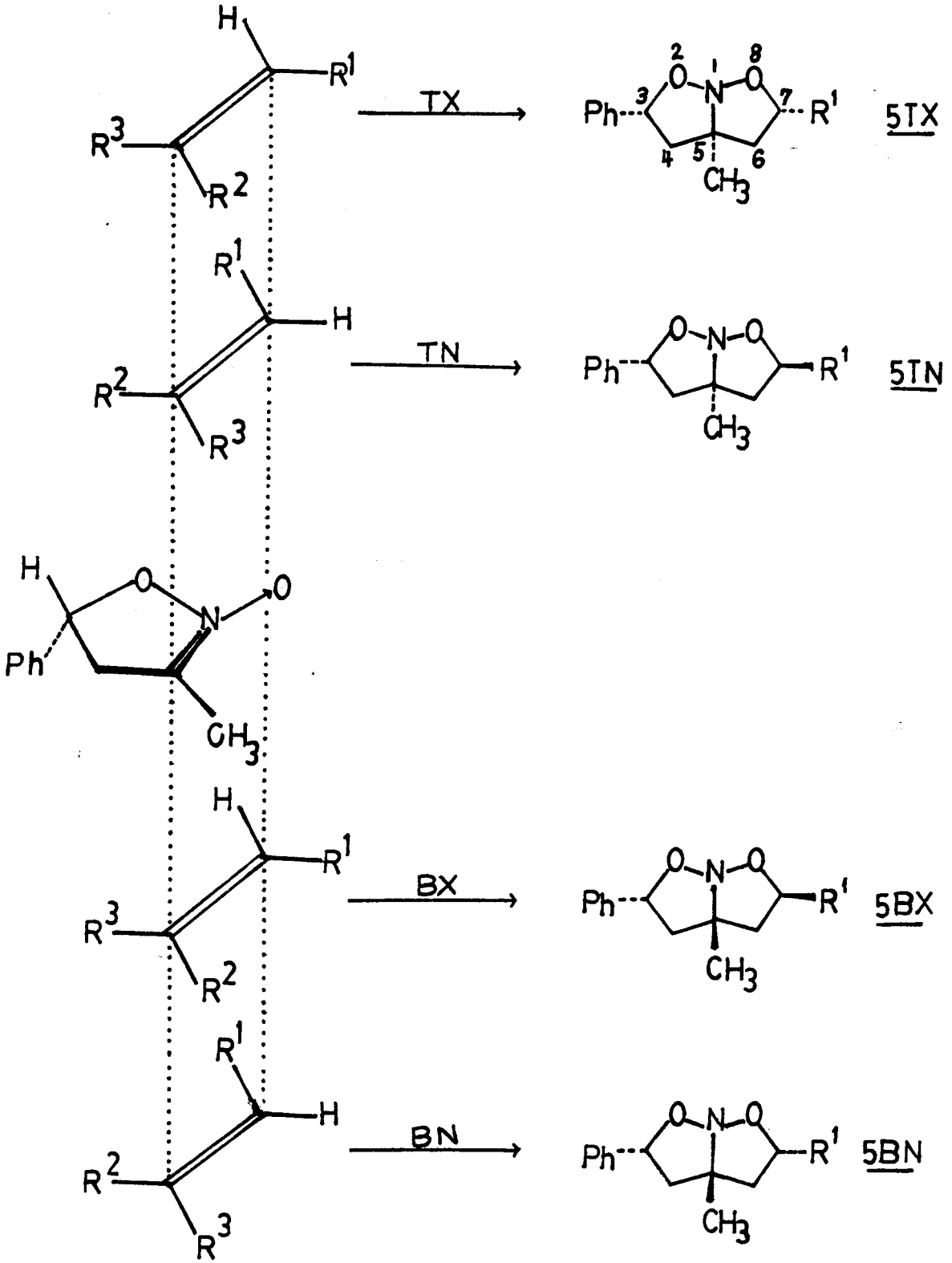

TABLE-2. RELATIVE YIELDS OF ADDUCTS FROM THE CYCLOADDITIONS OF 1 TO OLEFINS

ADDUCTS	RELATIVE YIELDS (%)			
	TX	TN	BX	BN
6	50	19	19	12[a]
7	54	46	0[c]	0[c]
8	51	18[b]	20[b]	11[b]
9	50	31	0[c]	19
10	71	14	10	5
12	65	0[c]	35	0[c]
11	15[b]	78	5[b]	2

a.Structures have not been assigned.

b.Assignments can be interchanged and structures have not been assigned.

c.Products could not be detected by NMR spectra.

The structures of these four diastereoisomers can be determined by analyzing the topological interrelationship of methyl, phenyl, and R^1 groups using proton NOE[33]. As shown in Table-14, the NOE experiments solved the stereochemistry of most of the cycloadducts. The ^{13}C NMR(see Table-10) signals were assigned with the aid of chemical shifts and intensities.

The infrared spectra(Table-11) showed typical O-N-O stretching absorption in the 1000 cm^{-1} region[28]. The UV spectra(Table-12) showed absorptions for a phenyl ring in the 250-270 nm region. Elemental analysis and MS by CI mode established the molecular formula. All of the cycloadducts showed abundant fragments of m/e at 77, 91, 104, 105 and 129 [34] for $C_6H_5^+$, $C_7H_6^+$, $C_8H_8^+$, $C_6H_5CO^+$ and the methyl-phenyl-cyclopropenoic cation 1B.

N-oxide 1 failed to react with trans-stilbene and vinyl acetate when heated for 90 hours and 9 days respectively. The reaction of N-oxide 1 with nitrosobenzene leaded to an unidentified product.

The experiment of the "test for kinetic vs. thermodynamic control" using cycloadducts 6BX and a mixture of cycloadducts 8TX + 8TN (in 3:1 ratio) showed no changes in the composition of the starting materials. These results clearly indicate that the cycloadditions are kinetically controled.

2a. Cycloaddition to Methyl Acrylate

Cycloaddition to methyl acrylate gave 3-phenyl-5-methyl 7-methoxycarbonyl-1-aza-2,8-dioxabicyclo[3.3.0]-octane. The crude product was separated by HPLC to yield pure 6TX, 6TN and 6BX. 6BN was obtained as an impure specimen contaminated by about 30% of 6TN.

SCHEME 2-2

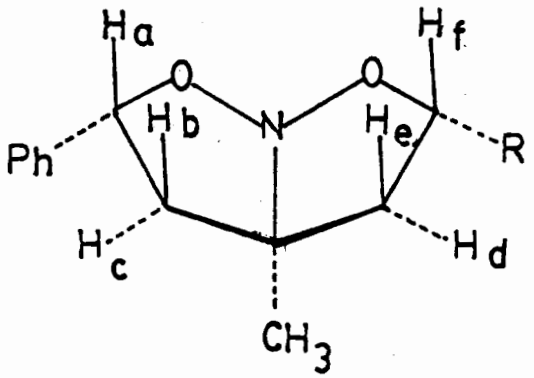

6,7,8 TX

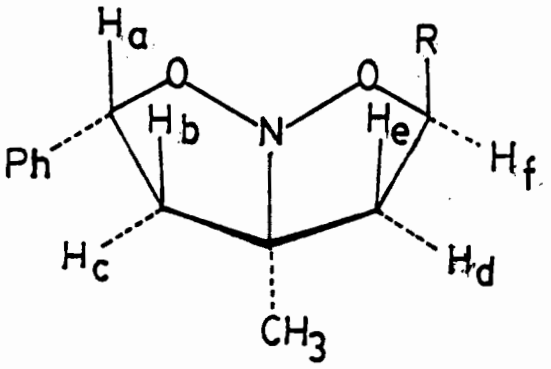

6,7,8 TN

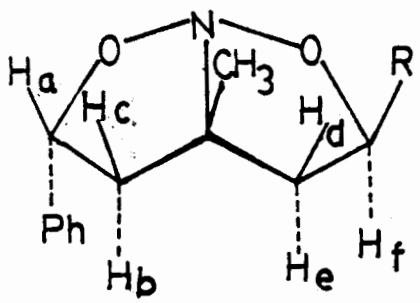

6,7,8 BX

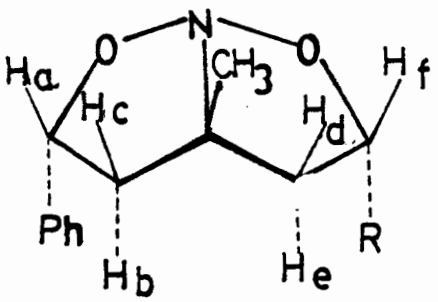

6,7,8 BN

R = 6, $COOCH_3$
7, Ph
8, CN

Irradiation of CH_3 resulted in a 2.7% and 2.1% enhancement of the H_c and H_d signals respectively on adduct 6TX and a 2.7% enchancement of the H_a, H_c and H_d signals on adduct 6BX. The results imply that H_c and H_d are oriented on the same side as the CH_3 group(see Scheme 2-2) in these two isomers and that H_a in 6TX is on the opposite side of the CH_3 while H_a in 6BX is on the same side of the CH_3. Irradiation of H_a resulted in a 5.8%, 1.4%, 1.7%, and 8.6% enhancement of the signals of H_b, H_c, H_e and H_f respectively, in 6TX and a 1.6% and 6.5% enhancement of the signals of H_b and H_c in 6BX. These results reveal that H_a is cis to H_b in the adduct 6TX and cis to H_c in the adduct 6BX. The observed large NOE effects between H_a and H_f in 6TX suggest that those protons are placed in close proximity through space[35]. This phenomenon can be explained by the steric compression arising from the bulky phenyl and methoxycarbonyl groups which would tend to pucker the two five-membered rings.

Irradiation of H_a in 6TN caused 5.9%, 3.9% and a weak enhancement of the H_b, H_e and H_c signals respectively. Irradiation of H_c and H_d both caused a weak enhancement of the CH_3 signal. These results ascertained that the positions of H_a, H_b and H_e are on the same side, and H_c, H_d and CH_3 are on the opposite side of the molecule. Irradiation of H_f caused a 6.3% enhancement of the H_d signal but not on the H_e signal.

Elemental analyses established the molecular formula of all the three isomers as $C_{14}H_{17}NO_4$. The IR spectrum of the cycloadduct showed absorptions typical of ester and O-N-O

groups: e.g. 1735, 1215 and 1005 cm^{-1} for 6TN, 1740, 1215, 1190 and 1020 cm^{-1} for 6BX, and 1735, 1215 and 1180 and 1015 cm^{-1} for 6TX. The MS by EI mode of the three isomers showed fragments at m/e 59(for $^{+}O{\equiv}C\text{-}OCH_3$), 77, 91, 104, 105, 129, 145 and 155 (for $M\text{-}C_6H_5\text{-}OCH_3$). Fragments 129 and 145 might arise by the following mechanism.

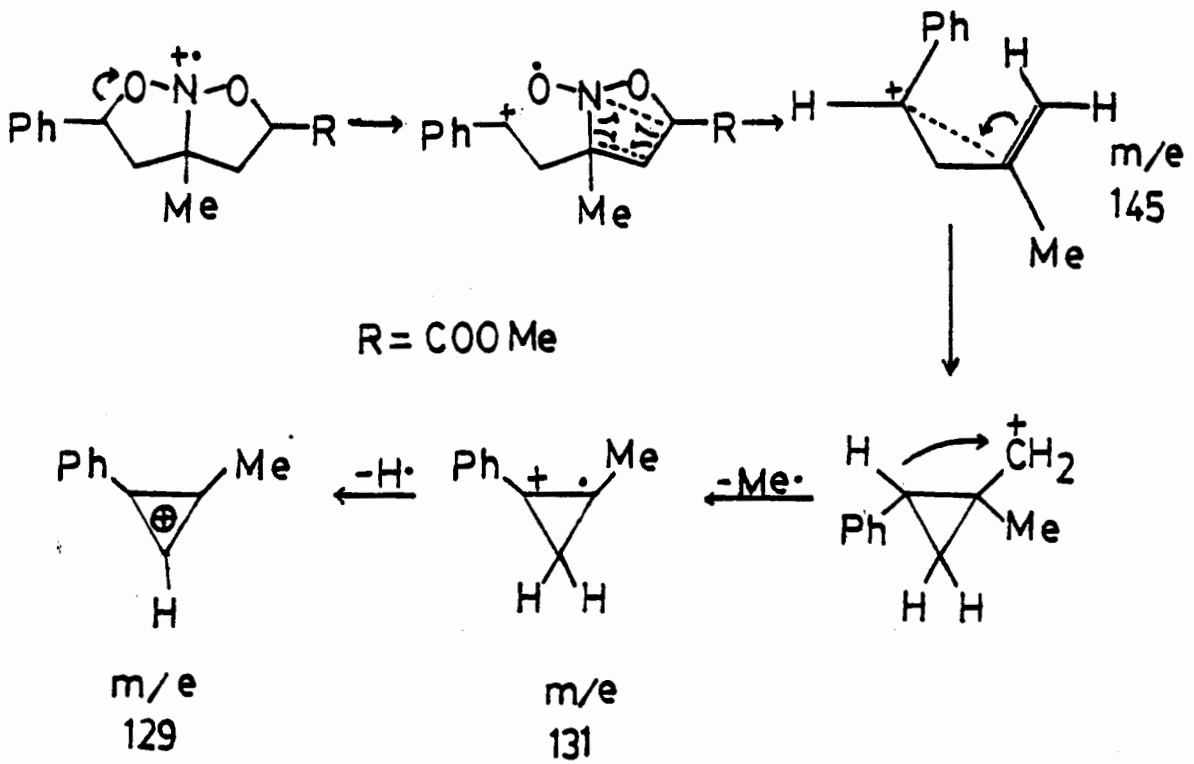

2b. Cycloaddition to Styrene

The heating of a solution of N-oxide 1 and styrene resulted in the formation of 3,7-diphenyl-5-methyl-1-aza-2,8-dioxabicyclo[3.3.0]-octane 7TX and 7TN. The NMR spectrum of 7TX showed a single , well resolved ABX splitting pattern at δ2.29, δ2.74 and δ 5.59 ppm. This indicates the presence of a plane of symmetry which cuts across the N-C-CH_3 axis: e.g. the magnetic environment of H_a-H_b-H_c is identical to that of H_d-H_e-H_f. Only 7TX and 7BN have these properties. The NOE data (Table-14.2) conclusively proves that it is 7TX, because the methyl and phenyl groups are located on the same side of the molecule.

The NMR data of 7TN showed two sets of ABX splitting patterns (Table-9). It can be seen from Table-14.2 that irradiation of CH_3 resulted in a 1.2% enhancement of the H_c signal, 1.3% of the H_d and 1.5% of the H_f. Irradiation of H_f resulted in a 7.5% enhancement of the H_d signal and had no effect on the H_e signal. This data suggests that H_c, H_d, and H_f are on the same side of CH_3. Irradiation of H_a caused a 3% enhancement on the H_b signal, 3.7% enhancement on the H_e signal, and no enhancement on the H_c signal. Therefore, H_a, H_b and H_e are on opposite side of the methyl group of the molecule.

In agreement with symmetry properties, 7TX displayed only four ^{13}C NMR signals(except for phenyl carbon signals) but 7TN gave six signals. Elemental analyses(Table-15) established the

molecular formula as $C_{18}H_{19}NO_2$ and the MS by CI mode gave an M+1 peak at m/e 282 for both cycloadducts. The MS by EI mode displayed similar fragment pattern for both isomers. 7TN and 7BX arising from top-endo and bottom-exo additions gave the same cycloadduct.

2c. Cycloaddition to Acrylonitrile

When heated a solution of N-oxide 1 and acrylonitrile yielded 3-phenyl-5-methyl-7-cyano-1-aza-2,8-dioxabicyclo[3.3.0]-octane, 8TX, 8TN, 8BX and 8BN. 8TX showed two sets of ABX splitting patterns(Table-9) and its NOE difference (Table-14.3) clearly indicates that the phenyl, methyl and cyano groups are oriented on the same side of the plane of the molecule. Irradiation of CH_3 of H_a confirmed that H_c and H_d are on the same side of the CH_3 and that H_a, H_b and H_f are on the opposite side. The fact that the enhancement of the signal for H_d was weaker than that of H_e, while it is saturating for H_f, suggests that H_e and H_f are cis to each other. The IR spectrum showed a weak absorbance at 2260 cm^{-1}, typical of a non-conjugated C≡N stretching vibration, and absorbance at 1045-960 typical of the O-N-O stretching mode. The MS by CI mode(iso-butane) gave an M+1 peak at m/e 231.

Another adduct tentatively assigned as 8TN was isolated together with 8TX in the ratio of 4:3(estimated by NMR) using

preparative HPLC. The ^{1}H and ^{13}C NMR spectra were obtained by subtracting the signals generated due to 8TX (see Table-9 and Table-10). The IR spectrum showed an absorbance at 2310 cm^{-1}, typical of C≡N band and at 1030 cm^{-1}, typical of an O-N-O band. The MS by CI mode gave an M+1 peak at m/e 231. The MS by EI mode showed m/e 77, 91, 104, 105 and 129 fragments. Elemental analysis established the molecular formula as $C_{13}H_{14}N_2O_2$.

Two more adducts, probably 8BX and 8BN, were isolated as a mixture by preparative HPLC(one peak). The ratio of the two isomers was 11:4(estimated by NMR). The ^{1}H and ^{13}C NMR data for the two isomers was obtained from the spectra of the mixture(Table-9 and Table-10). The I.R. spectrum of the mixture indicated the presence of a C≡N band at 2270 cm^{-1} and an O-N-O band at 1025-950 cm^{-1}. The MS(CI and EI mode) gave results similar to those of 8TX. The relative yields of the three unisolated isomers were 20%, 18% and 11%.

SCHEME 2-3

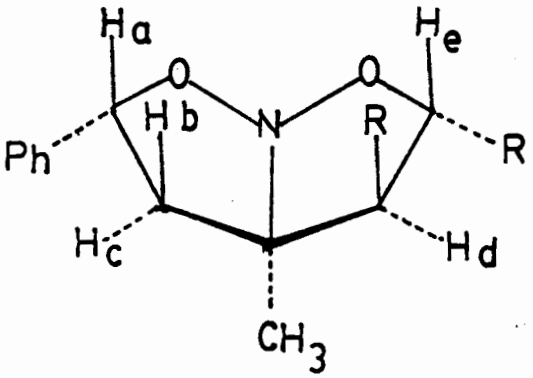

9,10TX

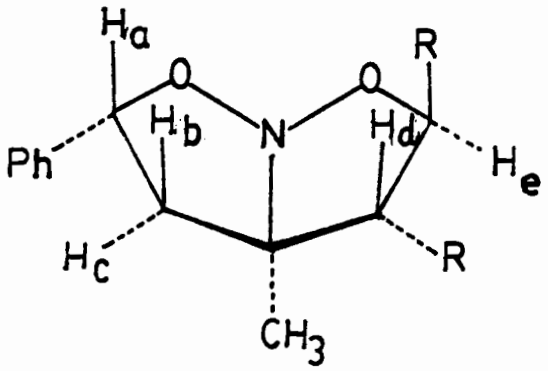

9,10TN

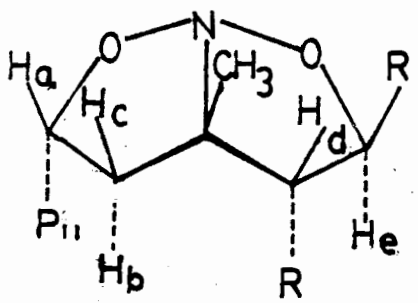

9,10BX

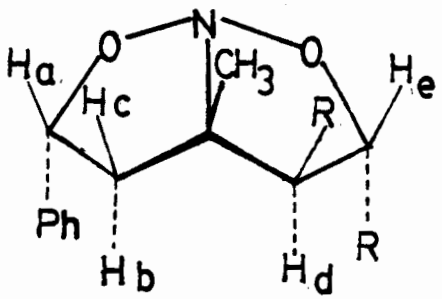

9,10BN

R= 9, $COOCH_3$
10, CN

2d. Cycloaddition to Dimethyl Fumarate

The heating of a solution of N-oxide 1 and dimethyl fumarate resulted in the formation of the cycloadducts 3-phenyl-5-methyl-6,7-dimethoxycarbonyl-1-aza-2,8-dioxabicyclo [3.3.0]-octane, 9TX, 9TN and 9BN(see Scheme 2-3).

Cycloadduct 9TX was isolated by preparative HPLC and showed ABX and AB coupling patterns in the ^1H NMR spectrum. The spatial relationships of the phenyl, methyl and two methoxycarbonyl groups were determined by NOE results(Table-14.4). The ^{13}C NMR spectrum(Table-10) showed two low field(170.18 and 169.71 ppm), low intensity carbonyl carbons and two methoxy carbons at 52.82 and 52.75 ppm. The I. R. spectrum showed absorbance at 1745, 1730, 1210 and 1180 cm^{-1}, characteristic of ester bands, and at 1020 cm^{-1}, the O-N-O stretching frequency. The MS by CI mode gave an M+1 peak at m/e 322. Elemental analysis established the molecular formula as $C_{16}H_{19}NO_6$.

Adduct 9TN was obtained in the pure state and showed ^1H NMR signals characteristic of one methyl, two methoxyl, one ABX pattern, and one AB pattern(Table-9). The NOE results and their interpretation was very similar to those of the NOE of 9TX. The larger effect of the proton H_e than H_c on irradiation of CH_3 might be explained by a twist of the five-membered ring by the large 7-methoxycarbonyl group. Other spectral data were comparable to those of 9TX, MS by EI mode showed common peaks at m/e 59, 77, 91, 104, 105, 129, 155((M+1)-(Ph)-(OCH_3)-($OCOCH_3$)),

171((M+1)-(Ph)-(CH_3)-($OCOCH_3$)), 199(M-(Ph)-3(CH_3)), 203(M-2($OCOCH_3$)), and 231(M-($OCOCH_3$)-(OCH_3)).

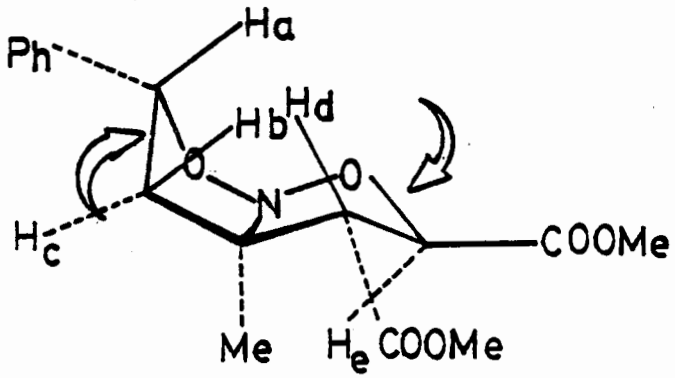

Adduct 9BN was obtained together with 9TX as a mixture in the ratio of 4:3. The spectral data and NOE results could be explained in a manner similar to that of 9TX and 9TN.

2e. Cycloaddition to Fumaronitrile

Heating of N-oxide 1 and fumaronitrile in acetonitrile resulted in the formation of the cycloadducts 3-phenyl-5-methyl-6,7-dicyano-1-aza-2,8-dioxabicyclo[3.3.0]-octanes, 10TX, 10TN, 10BX, and 10BN.

Cycloadduct 10TX was isolated by recrystalization and 10TN and 10BN were identified from a mixture of 10TX, 10TN, and 10BN in the ratio of 4:21:4. 10BX was identified from a mixture of adducts 10TX, 10TN, 10BX, and 10TN in the ratio of 3:4:32:1. NOE

results listed in Table-14.5 confirmed the structures of the 4 isomers shown in Scheme 2-3. Other spectral data were consistent with these structures.

The assignments of ^{13}C NMR are listed in Table-10. Adduct 10TX shows the cyano carbons at 114.86 and 114.63 ppm; adduct 10TN shows them at 114.87 and 114.14 ppm. All the samples gave M+1 peaks at m/e 256. Elemental analyses established the molecular formula for all of the samples as $C_{14}H_{13}N_3O_2$. Each I. R. spectra displayed a C=N band at 2252 cm^{-1} or 2260 cm^{-1}.

2f. Cycloaddition to Dimethyl Maleate

Heating of a solution of N-oxide 1 and dimethyl maleate resulted in the formation of 3-phenyl-5-methyl-6,7-dimethoxycarbonyl-1-aza-2,8-dioxabicyclo[3.3.0]-octane: 12TX and 12BX. The adduct 12TX was isolated as a pure specimen, and 12BX was isolated as a mixture with 12TX.

The ^1H NMR spectra of the two cycloadducts showed AB and ABX coupling patterns. Together with NOE results(Table-14.6) and other spectral data, the structures of 12TX and 12BX were confirmed. The MS by EI mode of both samples gave common fragments at m/e 59, 77, 91, 104, 105, 113, 129, 155, 171, 199, 203, and 231. The fragments m/e 185 and 262 might be explained as M-(Ph)-(CO_2CH_3) and M-(CO_2CH_3).

SCHEME 2 - 4

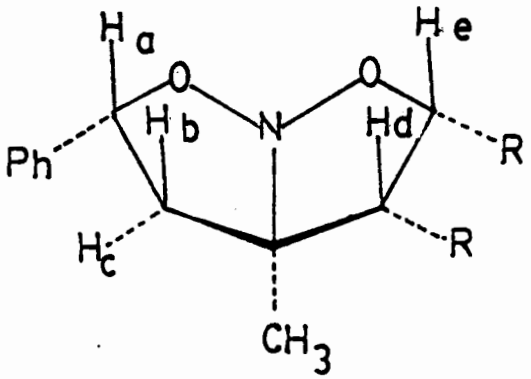

11,12 TX

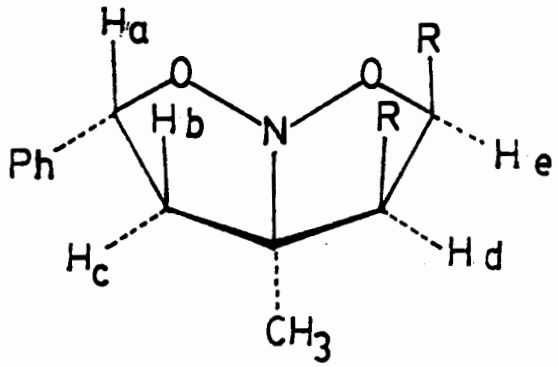

11,12 TN

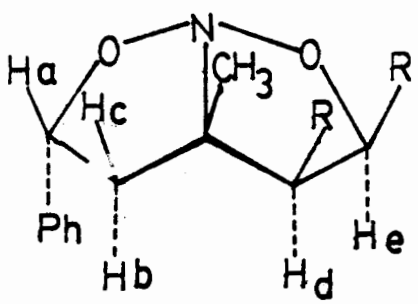

11,12 BX

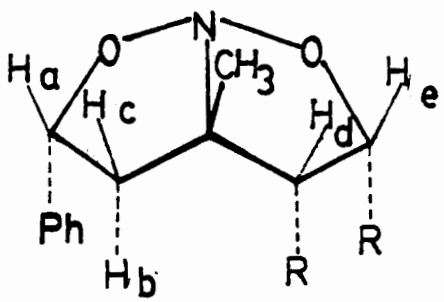

11,12 BN

11 , $(CO)_2O$ = R , R
12 , $COOCH_3$ = R

2g. Cycloaddition to Maleic Anhydride

Heating a solution of N-oxide 1 and maleic anhydride resulted in the formation of the cycloadducts 11TN, 11BN, and other products which could be 11TX and 11BX. The tailing of maleic anhydride and products on TLC and HPLC might be casused from the hydrolysis of the anhydride moiety. Adduct 11TN was obtained from recrystallization with CH_2Cl_2 as a mixture with 11BN in the ratio of 17:3. The ^1H NMR spectrum of the mixture showed major and minor sets of ABX and AB coupling patterns arising from the major and minor isomers. The I. R. spectrum of the sample showed absorptions 1790 cm^{-1} (C=O) and 995 cm^{-1} (O-N-O). The MS by CI mode gave the M+1 peak at m/e 276. Elemental analysis of this sample established the molecular formula as $C_{14}H_{13}NO_5$. The fragments from MS by EI mode were (m/e) 77, 91, 104, 105, 129, 171, and 173.

Irradiation of the methyl group of 11TN and 11BN, separately, caused enhancements of the H_c and H_d. The relative positions of the H_a, H_b, and H_c over the space of 11TN were readily determined by NOE %(Table-14.7), which showed that H_a is closer to H_b than to H_c. Irradiation of the H_d or H_e in 11TN and 11BN caused no effect on H_a, H_b or H_c in either case. This indicates that these two protons are in the exo orientation.

2h. Reaction of 1 with Nitrosobenzene

When 1 was added to a nitrosobenzene solution(acetone) at room temperature, the color of the solution changed gradually from blue to yellow then to red, producing a red oil. The yellow solution consisted of one new product and N-oxide 1; the red solution included predominantly the new product(This was determined by NMR measurements: both of the yellow and red solutions have NMR spectra gave easily distinguishable sharp signals.). The new product contained one singlet methyl signal, three double-doublet signals(in ABX pattern) and a 10 proton phenyl multiplet signal. The singlet methyl signal was the same as that of the other cycloadducts. This fact might suggest that a new bond is formed at C-3 on N-oxide 1. The ESR of the red solution(Figure 4-2) exhibited a multiplet of triplet signals with g=2.0078 and a=10.25 G. Comparing these values with the cases of nitroxide derivatives($PhNC(O\bullet)CHRR^1$, $a_N \simeq 10$ G) reported by Eaton, indicate that the product might be a nitroxide. IR absorptions(see experimental section) suggest that the new product might contain an N-H moiety.

3. Cycloadditions Under High Pressure

The results and conditions of the cycloadditions to methylacrylate, dimethylfumarate, fumaronitrile and maleic anhydride under high pressure at room temperature(22° C) are summarized in Table-3. The relative percentages of cycloadducts were calculated from the integration of NMR signals. For cycloadducts 9 the integrations of the Hd signals at 3.73 ppm(9TX), 3.98 ppm(9TN), and 3.90 ppm (9BN) were used. For other cycloadducts, CH_3 signals were integrated.

Table-3. The cycloaddition of N-oxide 1 to olefins under high pressure (22°C).

adducts	%conversion of 1	ratio of adducts(%)[a] TX	TN	BX	BN	conditions
9	100%	63	25	0[b]	12	2.07KBar,240h
	(100%)	(50	31	0[b]	19)	85°C,432h
10	100%	87	7	4	2	1.38Kbar,54h
	(100%)	(71	14	10	5)	82°C,168h
11	93%	18	82	0[c]	0[c]	1.38KBar, 6h
	(100%)[d]	(15[e]	78	5[e]	2)	82°C,8h
6	100%	46	19	24	11	2.07KBar,50h
	(100%)	(50	19	19	12)	50°C, 93h

a. Those figures in parenthesis are the results taken under 1 bar.

b. not detected by NMR spectroscopy.

c. Small amount was detected which could not be integrated.

d. Percentage conversion of maleic anhydride.

e. These assignments can be interchanged.

4. Formation Constants of Ground State Complexes

Charge transfer(CT) electronic transitions of donor-acceptor complexes were discovered in the 1950's by Mulliken[36]. The application of the UV spectrophotometric method for the analysis of CT absorption spectra and the evaluation of the absorptivity of the complex(ϵ_{CT}) and the equilibrium constant(K) was discussed in detail by Briegleb[37].

The K value of the complex of maleic anhydride with 1 was obtained from equation {1} in which we assumed that the optical density of 1 at the monitoring wavelength and concentration can be neglected. The K value of the complex of fumaronitrile and trans-stilbene with 1 was obtained from equation {2}. We assumed that the optical density of trans-stilbene did not change.

Preliminary experiments provided the following information:

1. 0.075 M of dimethyl maleate(DMM) and 0.075 M of N-oxide 1 (CN): no significant change of absorbance in the range of 280 - 500 nm.
2. 0.075 M of dimethyl fumarate(DMF) and 0.075 M of CN: no

significant change in the range of 290-500 nm.

3. 0.075 M of fumaronitrile(FN) and 0.075 M of CN: a significant change at λ=267 nm where the absorbance of FN is zero and that of CN is 1.30, and the observed absorbance is 1.37.
4. 0.00075 M of trans-stilbene(SB) and 0.00075 M of CN: at 307 nm, the absorbance of SB is 1.99 and that of CN is zero, and the observed absorbance is 2.10.
5. 0.075 M of vinyl acetate(VA) and 0.075 M of CN: no significant change in a range of 260-500 nm.
6. 0.02 M of maleic anhydride(MA) and 0.0001 M of CN: at 306 nm, the absorbance of MA is 0.318 and that of CN is zero, and the observed absorbance is 0.327.

4a. Maleic Anhydride

For the reaction of CN and MA, if i)the concentrations are $a_0 >> b_0$, and (ii) the O. D. of CN at the examining wavelength (300nm) is negligible, K can be defined as shown below from which equation {1} can be derived.

$$MA + CN \underset{}{\overset{K}{\rightleftharpoons}} CT$$

a_o	b_o		before equilibruim
a_o	b	b_o-b	after equilibrium

The equilibrium constant = $K = (b_o-b)/a_o b$. The concentration of a_o can be assumed to be constant.

We define that ϵ_1: molar absorptivity of MA

ϵ_2: molar absorptivity of complex

A': observed absorbance

$$b = b_o / (K \times a_o + 1)$$

$$A' = [\epsilon_2 \times (b_o-b) \times l] + (\epsilon_1 \times a_o \times l)$$

$$= (\epsilon_2 \times b_o \times l) - [\epsilon_2 \times b_o \times l / (K \times a_o + 1)] + A_o$$

where $A_o = \epsilon_1 \times a_o \times l$

$$\Delta A = A' - A_o$$

$$= K \times a_o \times \epsilon_2 \times b_o \times l / (K \times a_o + 1)$$

we obtain,

$$1/\Delta A = (1 / \epsilon_2 \times b_o \times l) + (1/\epsilon_2 \times b_o \times l)(1/K)(1/a_o) \quad \{1\}$$

Plotting of $1/\Delta A$ vs $1/a_o$ should give a straight line with the slope=$(1/\epsilon_2 x b_o x l)(1/K)$ and the intercept= $1/\epsilon_2 x b_o x l$, from those

relations both K and ϵ_2 can be calculated.

For the ground state complex formation of maleic anhydride and N-oxide 1, following data (TABLE-4) were obtained with [1]=1.02 x 10^{-4} M; optical density $\simeq$ 0 at 300nm.

TABLE-4. OPTICAL DENSITIES OF GROUND STATE COMPLEX BETWEEN 1 AND MA AT DIFFERENT CONCENTRATIONS OF MA.

$[MA]=a_o$	A_o	A'	$1/\Delta A$
0.02M	0.318	0.327	111
0.016M	0.257	0.265	125
0.0096M	0.149	0.155	167
0.0048M	0.072	0.076	250

The plotting of $1/\Delta A$ vs $1/a_o$ is given in Figure 2-1 in which the calculated slope=0.871 and the intercept=70.67 with the correlation coefficient(γ) of 0.998. The K$\simeq$81 M^{-1}, and $\epsilon_2 \simeq 140$. The UV absorptions is shown in Figure 2-2.

Figure 2-1. Plot of $1/\Delta A$ vs. $1/a_0$ for the ground state complex formation constant of maleic anhydride and N-oxide 1.

slope = 0.871

intercept = 70.67

corr. coeff. = 0.998

$K \simeq 81\ M^{-1}$

$\epsilon_2 \simeq 140$

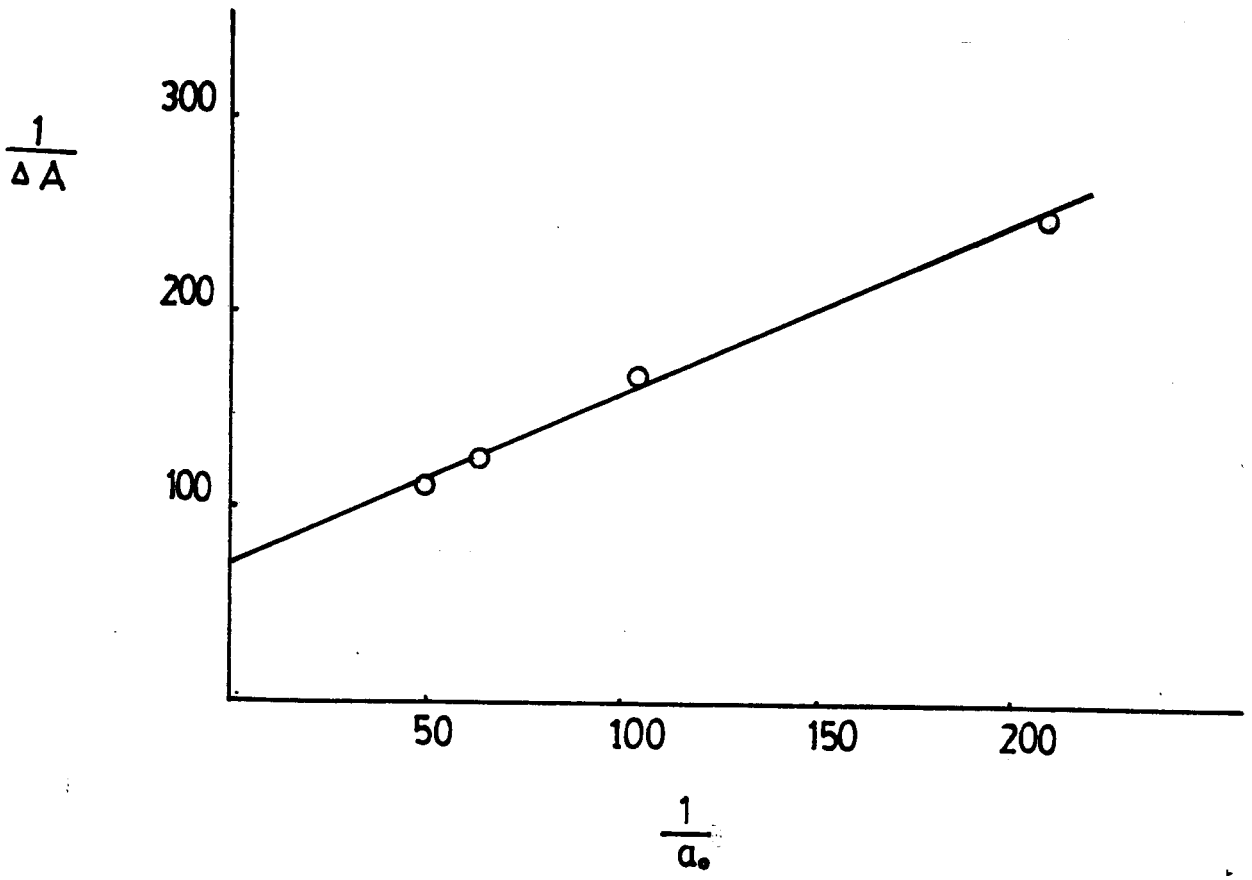
1/ΔA
300
200
100
50
100
150
200
1/a₀

Figure 2-2. The UV absorptions of the ground state complex between 1 and MA at different concentrations of MA

1. [1]=.000102M
2. .02M MA
3. .02M MA + [1]
4. .016M MA
5. .016M MA + [1]
6. .0096M MA
7. .0096M MA + [1]
8. .0048M MA
9. .0048M MA + [1]

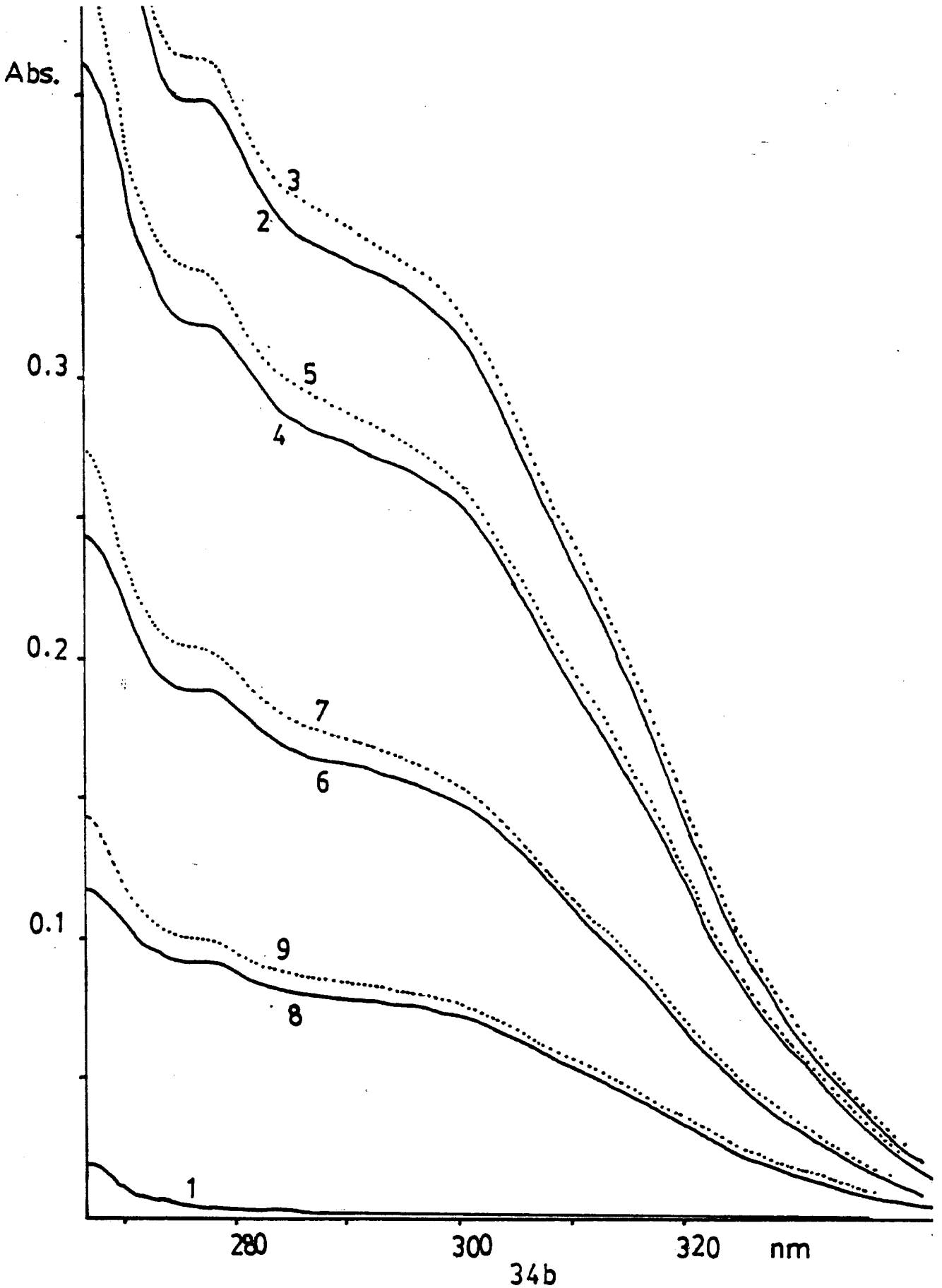

34b

4b. Fumaronitrile

To determine the K value of fumaronitrile(FN) and N-oxide 1(CN) equation {2} was used[38]. Equation {2} can be obtained under the following conditions:

(i) $a_o >> b_o$, and

(ii) the absorption of FN does not change after equilibrium is reached.

$$FN + CN \underset{}{\overset{K}{\rightleftharpoons}} CT$$

a_o	b_o		before equilibrium
a_o	b	$b_o - b$	after equilibrium

We define that ϵ_3: molar absorptivity of CN

ϵ_2: molar absorptivity of complex

A_4: absorbance of FN only

A': observed absorbance of the solutions

$\epsilon = A/b_o \times l$

(l=0.1cm)

$A = A' - A_4$

$$a_o/(\epsilon-\epsilon_3) = a_o/(\epsilon_2-\epsilon_3) + [1/(\epsilon_2-\epsilon_3)](1/K) \quad \{2\}$$

The following data (TABLE-5) data were obtained with [1]=1.5 X 10^{-2} M, and ϵ_3=170 at the examining λ (267nm).

TABLE-5. OPTICAL DENSITIES OF GROUND STATE COMPLEX BETWEEN 1 AND FN AT DIFFERENT CONCENTRATIONS OF FN.

$[FN]=a_0$	A_3	A_4	A'	ϵ	$[a_0/(\epsilon-\epsilon_3)]\times10^6$
3.0 M	0.255	0.590	1.270	453	10601
2.7 M	0.255	0.531	1.180	433	10266
2.4 M	0.255	0.472	1.086	409	10042
2.0 M	0.255	0.393	0.958	377	9662
1.8 M	0.255	0.354	0.892	359	9524
0.0	0.255	---	0.255		

The plot of $a_0/(\epsilon-\epsilon_3)$ vs. a_0 is shown in Figure 2-3, from which the slope=$1/(\epsilon_2-\epsilon_3)$=894 x 10^{-6} and the intercept=$1/(\epsilon_2-\epsilon_3)K$=7890 x 10^{-6}. The K and ϵ_2 are determined to be 0.11M^{-1} and 1289, respectively. The UV absorptions is shown in Figure 2-4.

Figure 2-3. Plot of $a_0/(\epsilon-\epsilon_3)$ vs. a_0 for the ground state complex formation constant of fumaronitrile and N-oxide 1.

slope = 894×10^{-6}

intercept = 7890×10^{-6}

corr. coeff. = 0.9978

$K \simeq 0.11\ M^{-1}$

$\epsilon_2 \simeq 1289$

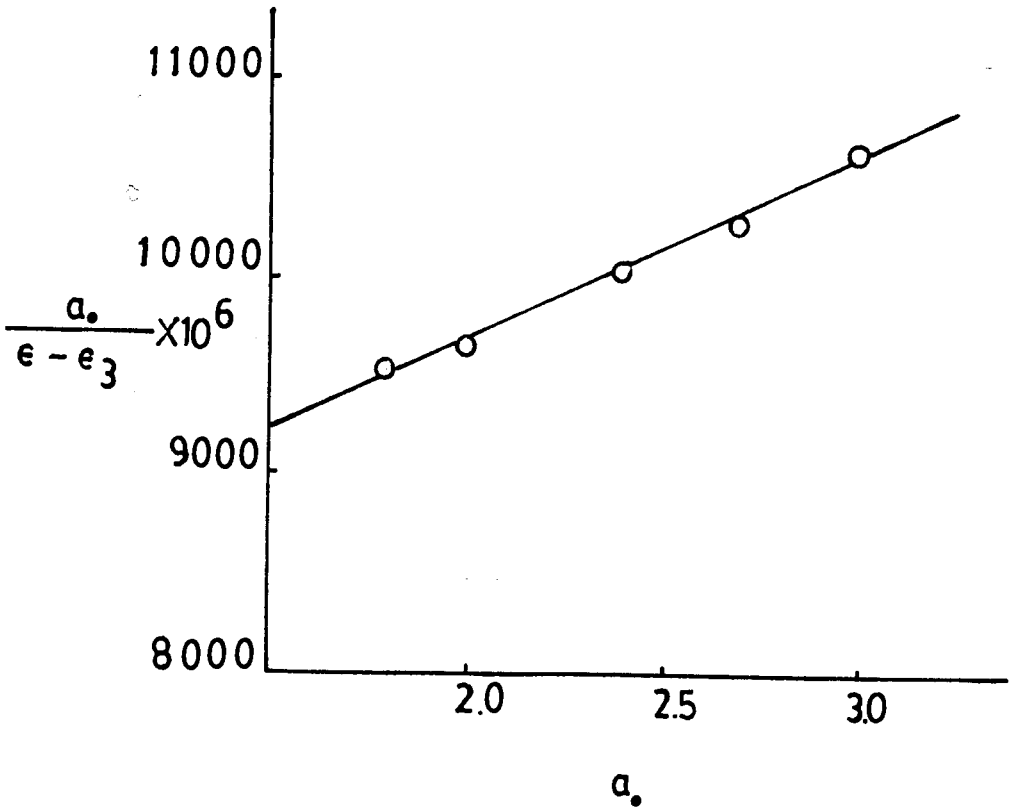
11000
10000
9000
8000
$\frac{a_0}{\epsilon - e_3} X10^6$
2.0
2.5
3.0
a_0

figure 2-4. THE UV ABSORPTIONS OF THE GROUND STATE COMPLEX BETWEEN 1 AND FN AT DIFFERENT CONCENTRATIONS OF FN.

1. [1]=.015M
2. 3.0M FN
3. 3.0M FN + [1]
4. 2.7M FN + [1]
5. 2.4M FN + [1]
6. 2.0M FN + [1]
7. 1.8M FN + [1]

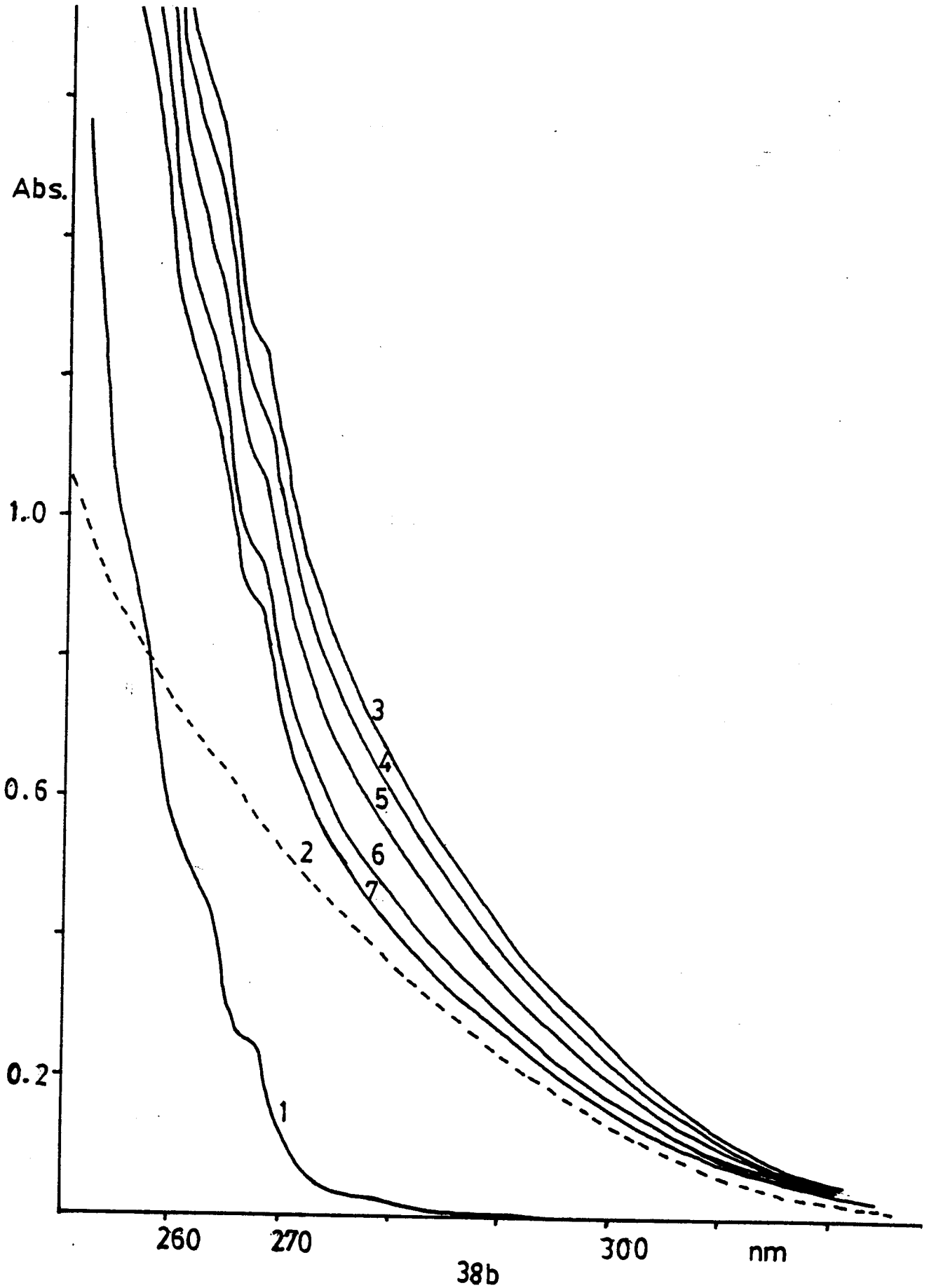

38b

4c. trans-Stilbene

The equilibrium expression for the reaction of SB with 1 is shown below. The examining λ was 294 nm where we assumed (i) [CN]>>[SB], (ii) the concentration of CN remained constant after equilibrium was reached and hence the absorption of CN could be subtracted from the observed absorbance to give the difference absorbance A. Equation {2} can be applied to this measurement.

$$SB + CN \underset{}{\overset{K}{\rightleftharpoons}} CT$$

b_o	a_o		before equilibrium
b	a_o	b_o-b	after equilibrium

$$K = (b_o-b)/a_o b$$

The following data (TABLE-6) were obtained with

b_o=[SB]=5 x 10^{-4} M and ϵ_5=34600 in all cases. Where we define that:

A_3 : absorbance of CN only

A' : observed absorbance of the solutions

$A = A' - A_3$

$\epsilon = A/b_o \times l$

ϵ_5 : molar absorptivity of SB

TABLE-6. OPTICAL DENSITIES OF THE GROUND STATE COMPLEX BEYWEEN 1 AND SB AT DIFFERENT CONCENTRATIONS OF 1

$[CN]=a_o$	A_3	A'	A	ϵ	$[a_o/(\epsilon-\epsilon_5)] \times 10^6$
0.075M	0.030	1.780	1.750	35000	187.5
0.060M	0.024	1.774	1.750	35000	150.0
0.045M	0.018	1.766	1.748	34960	125.0
0.030M	0.012	1.758	1.746	34920	93.8
0.015M	0.006	1.748	1.742	34840	62.5

The plot of $a_o/(\epsilon-\epsilon_5)$ vs. a_o is given in Figure 2-5, from which the slope[$1/(\epsilon_2-\epsilon_5)$]= 2042 x 10^{-6}, the intercept [$1/(\epsilon_2-\epsilon_5)K$] =3.19 x 10^{-6}, and γ=0.998 (correlation coefficient): K $\simeq$ 60 and $\epsilon_2 \simeq$ 35090.

Figure 2-5. Plot of $a_0/(\epsilon-\epsilon_s)$ vs. a_0 for the ground state complex formation constant of trans-stilbene and N-oxide 1.

slope = 2042×10^{-6}

intercept = 3.19×10^{-6}

corr. coeff. = 0.998

K $\simeq$ 60

ϵ_2 $\simeq$ 35090

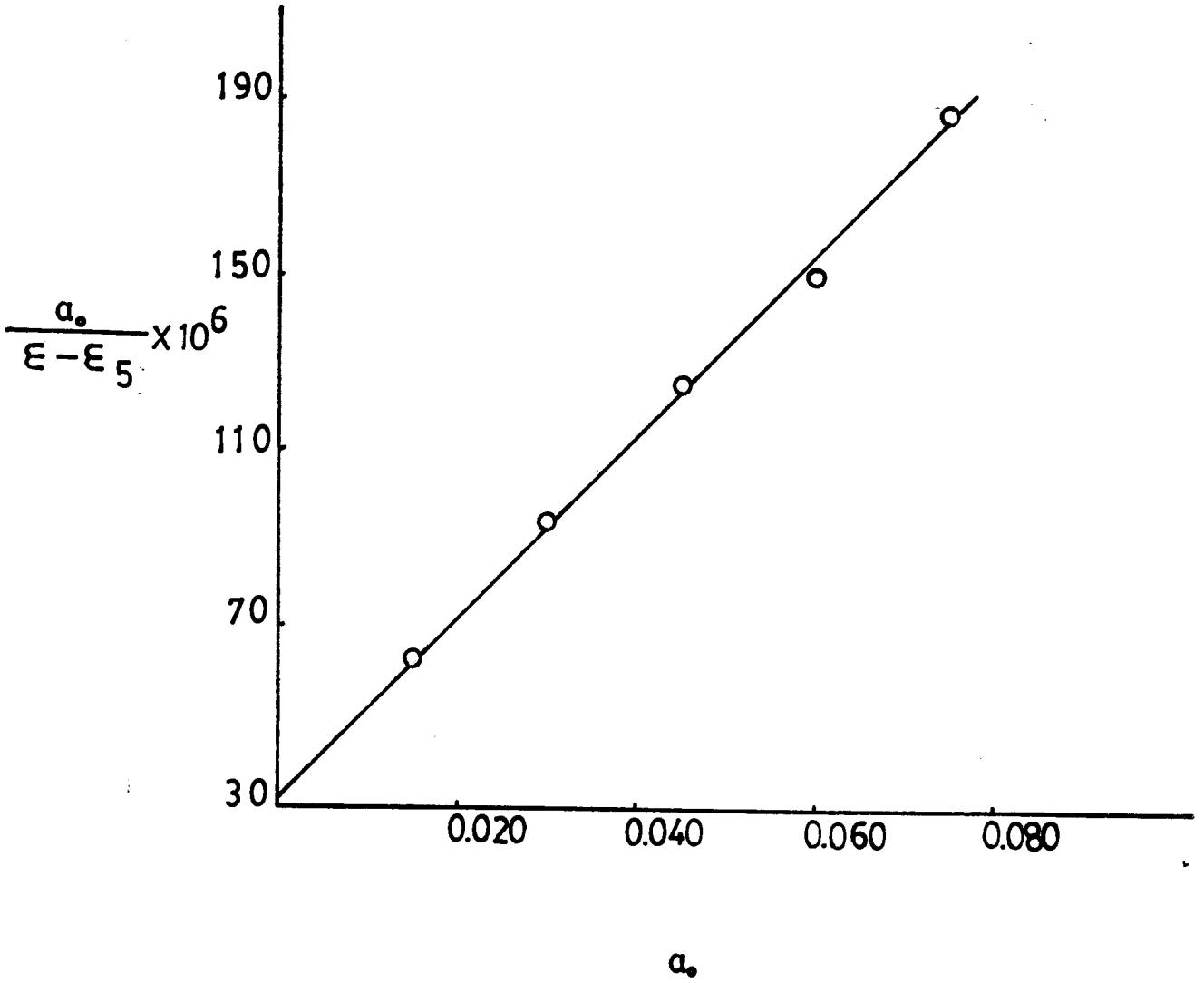
190
150
110
70
30
$\frac{a_0}{\varepsilon - \varepsilon_5} \times 10^6$
0.020
0.040
0.060
0.080
a_0

4d. Vinyl Acetate

The lack of reactivity of VA with N-oxide 1(CN) might be caused by the electron-donating acetate group. Measurements of the ground state complex were made for different concentrations of vinyl acetate over a wide range (250-500 nm) and no change of the spectra was observed. The following measurements (TABLE-7) were taken at 267 nm at which the absorbance of 0.0075 M CN was 0.136 and the absorbance of VA nil.

TABLE-7. OPTICAL DENSITIES OF THE SOLUTIONS OF VA AND 1 AT DIFFERENT CONCENTRATIONS OF VA

[VA](M)	[CN](M)	A'
1.086	0.0075	0.137
0.869	0.0075	0.136
0.625	0.0075	0.135
0.543	0.0075	0.139
0.217	0.0075	0.135
0.109	0.0075	0.136

CHAPTER 3

Discussion

The observations of 1,3-dipolar cycloadditions to N-oxide 1 allow us to draw the following conclusions:

1. The cycloaddition to mono-substituted olefins gives only one regioisomer 3 in all cases.
2. The top-exo type adducts are the major products in every cycloaddition except for the reaction of N-oxide 1 with maleic anhydride which gives predominantly a top-endo cycloadduct.
3. The chemical shifts of H_c are always recorded at a higher field than those of H_b in TX-type and TN-type cycloadducts; the chemical shifts of H_b are always at a higher field than those of H_c in BX-type adducts.
4. $J_{ab} < J_{ac}$ in most of the TX- and TN-type adducts, and $J_{ac} < J_{ab}$ in most of the BX- and BN-type adducts.
5. The cycloadditions of di-substituted olefins , fumaronitrile and dimethyl fumarate, under high pressure resulted in an increase in the relative yields of the major product.

1. Stereochemistry

Four diastereoisomers could be obtained from the four different approaches of dipolarophile to N-oxide 1. The relative yields of the cycloadducts are summarized in Table-2.

1a. Mono-Substituted Olefins

The cycloadditions of 1 with three mono-substituted olefins occur primarily by the TX approach which is the least hindered pathway from steric arguments. The second favorable pathway should be TN or BX approaches. By the TN pathway, there might be a slight interaction between the substituted group in the olefins and the five-membered ring of N-oxide 1. By the BX pathway, there might be steric hindrance between the olefins and the phenyl group in the N-oxide 1. The degree of the two steric effects should be dependent on the geometry of substrate approaches and the size of the substituent group in the olefins. The cycloadditions with methyl acrylate and acrylonitrile gave similar results. The ratios of 6TN/6BX and 8TN/8BX are nearly unity. The fact that the BN approach is the least favored is reflected by the low yields of the products 6BN(12%), 7BN(≃0%) and 8BN(11%). The steric repulsions can arise not only from interactions between the substituents on the olefin and the 5-membered ring of 1 but also from the 5-phenyl group in 1 and substituents on the olefins.

The steric interactions of substituent groups in olefins and 5-substituted 3-nitro-isoxazoline N-oxide have been discussed[27](Scheme 3-1). Although the isomers have not been identified and structure not been assigned (two peaks in GLC spectra were observed), we interpret the stereochemistry of the products as shown. It seems that the steric effects from olefin substituents are larger than those effects from the 5-substituent in isoxazoline N-oxide.

SCHEME 3-1

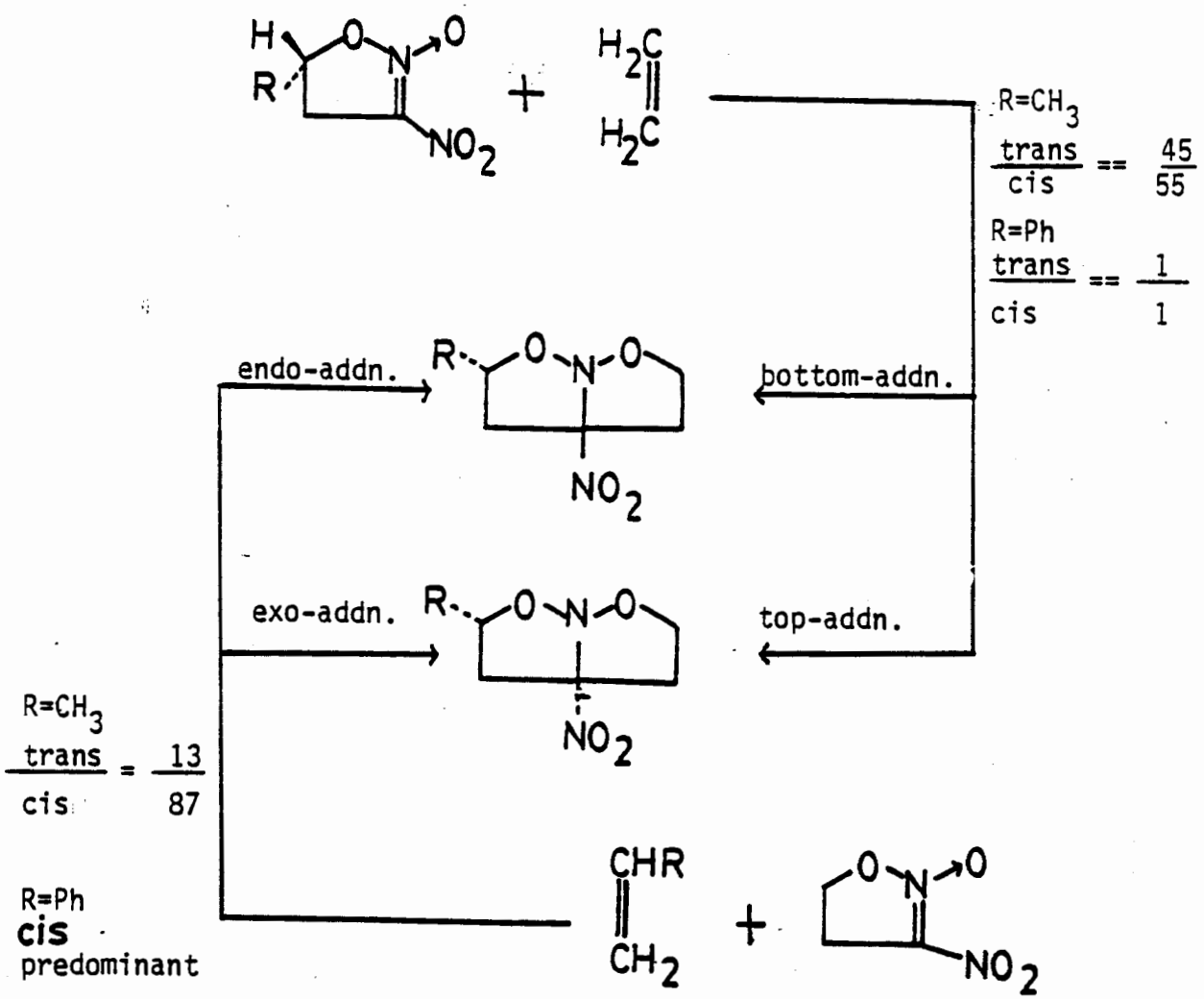

1b. trans-Olefins

The steric effect of the cycloaddition of trans-olefins to N-oxide 1 is more complicated than those of mono-substituted olefins. The steric interactions not only arise from the substituents in the olefins but also from the five-membered ring and 3-methyl group in 1. The approach from the top must be much easier than approach from the bottom because of the position of the 5-phenyl group in 1. As shown in Scheme 2-1, in the TX approach there is steric interaction between R^3 and the five-membered ring, and in the TN approach the steric interaction is a sum of R^1 with the five-membered ring and R^3 eclipsing the 3-methyl group on 1. These interactions are also dependent on the size of angle θ(Figure 3-1). The results show that the TX approach is more favorable than the TN one. It is obvious that the sum of the steric interactions between R^3 and the 5-methyl group and between R^1 and the five-membered ring(TN approach) is larger than the interactions between R^3 and five-membered ring(TX approach). The fact that the ratio of 10TX/10TN(=71/14) is larger than that of 9TX/9TN(=50/31) indicates the balance of the two effects due to the size of the substituents on the olefins. It appears that in the former the interaction of the CN with the CH_3 dominates, and in the latter that of the methoxycarbonyl group with the five-membered ring dominates the balance of steric effects.

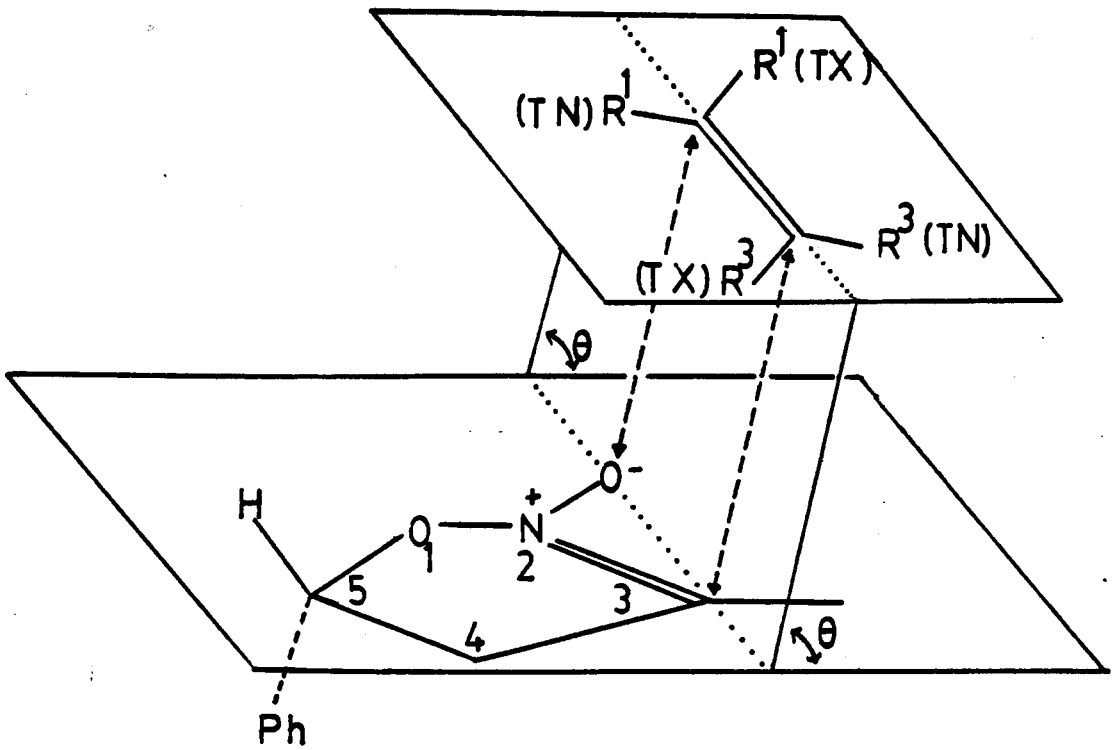

Figure 3-1. Model of the approach of olefin to N-oxide 1.

In the approach from the bottom, a large steric interaction arises from the 5-phenyl group in 1. This is counter balanced somewhat by the interaction with the methyl group. While dimethyl fumarate prefers BN pathway, fumaronitrile prefers the BX pathway. It appears that the phenyl group interacts less with the cyano group on R^3 than with the methoxycarbonyl on R^3.

1c. cis-Olefins

The cycloaddition of dimethyl maleate gave only the exo-adducts (12TX and 12BX) and no endo-adducts(12TN and 12BN) because of the steric effects of the R^1 and R^2 groups (see Scheme 2-1, R^3=H). However, that of maleic anhydride gives the TN-adduct as the predominant species(11TN, 78%). This indicates that the steric hindrance is not the major controlling factor in this particular case. In this case, the endo transition state possesses secondary orbital interactions which favor this approach over its exo counterpart. This phenomenon has been explained by Padwa[39] in the cycloaddition of nitrones to olefins, and also by Gree and Carrie[40] in their studies of exo/endo ratios of nitronic ester cycloadditions with olefins. This will be discussed by the frontier orbital theory later in this thesis.

2. Regiochemistry

In section 2-1, it was mentioned that there are two possible regioisomers(3 and 4) which might be obtained from the cycloadditions of N-oxide 1 to mono-substituted olefins. This phenomenon has also been discussed by Coates[41] in terms of frontier orbital theory. The results of the cycloadditions of nitronic esters reported by Shimizu[32] and Tartakovskii[42] gave only regioisomer 3. The regiochemistry of the cycloaddition was discussed by Huisgen[2] on the basis of electronic and steric effects, the latter usually being the dominant factor. The present cycloaddition to mono-substituted olefins yields products 6, 7, 8. and can be explained by the tendency to minimize the repulsion between the methyl group on N-oxide 1 and the substituent on olefin.

3. The Frontier Orbital Theory of Cycloadditions

The interpretation of 1,3-dipolar cycloadditions of nitronic esters to α,β-diactivated olefins and monodeactivated olefins by frontier orbital theory has been widely discussed by Gree and co-workers[43]. MO calculations of many different kinds of 1,3-dipoles have also been done by Houk[44,45]. Fleming has also used the theory to deal with the reaction rates, as well as

the stereo- and regio-chemistry of the thermo pericyclic reactions[46,47]. The reactivities of 1,3-dipoles and dipolarophiles can be rationalized in terms of frontier molecular orbital theory. The rate of reaction is dependent on the energy difference between LUMO(dipole)-HOMO(dipolarophile) and/or HOMO(dipole)-LUMO(dipolarophile) while the regiochemistry is dependent on the control of the dipole LUMO or dipole HOMO[47] (see Figure 3-2).

The first step in predicting the frontier orbital interaction is the choice of a suitable HOMO/LUMO pair of 1,3-dipole and olefin (Figure 3-3 and TABLE-8). The second step is to estimate the relative size of the coefficients of the atomic orbitals from the chosen HOMO/LUMO pair. The third step is to match up the large coefficient of one component with the large coefficient of the other and the small one matchs the small one [50].

Both the 3-methyl group and the 1-oxygen atom on N-oxide 1 release electron density into the π system of the nitronic ester, thereby raising the HOMO and LUMO energy levels of this 1,3-dipole. In olefins, electron-withdrawing groups lower their HOMO and LUMO energies. These effects tend to lower the HOMO-LUMO energy gap between N-oxide 1 and the olefins as shown in Figure 3-2(a)[50].

In comparing the geometric structure of all the olefins, maleic anhydride seems to have the most suitable array of π-orbitals for secondary interaction with the orbitals on 1,3-dipole (Figure 3-4) [51]. The orientations of the dipole moments of these two substrates also establish the favorable transition state of the addition reaction. This interaction probably gives rise to a strong ground state complex formation as observed.

The much slower rate of the cycloaddition of 1 to dimethyl maleate than to dimethyl fumarate may be caused by the increasing steric repulsion between the two methoxycarbonyl groups during the hybridization change from sp^2 to sp^3 of the central carbon atoms of the maleate. The C-C bond distance is somewhate lengthened, but the attendant shrinkage of the bond angle from 120° to 109° results in considerable compression of the Van der Waals radii of the eclipsed cis-substituents (Figure 3-5) [2]. This leads in turn to a higher activation energy for the cycloaddition to the cis isomer than that to the trans isomer.

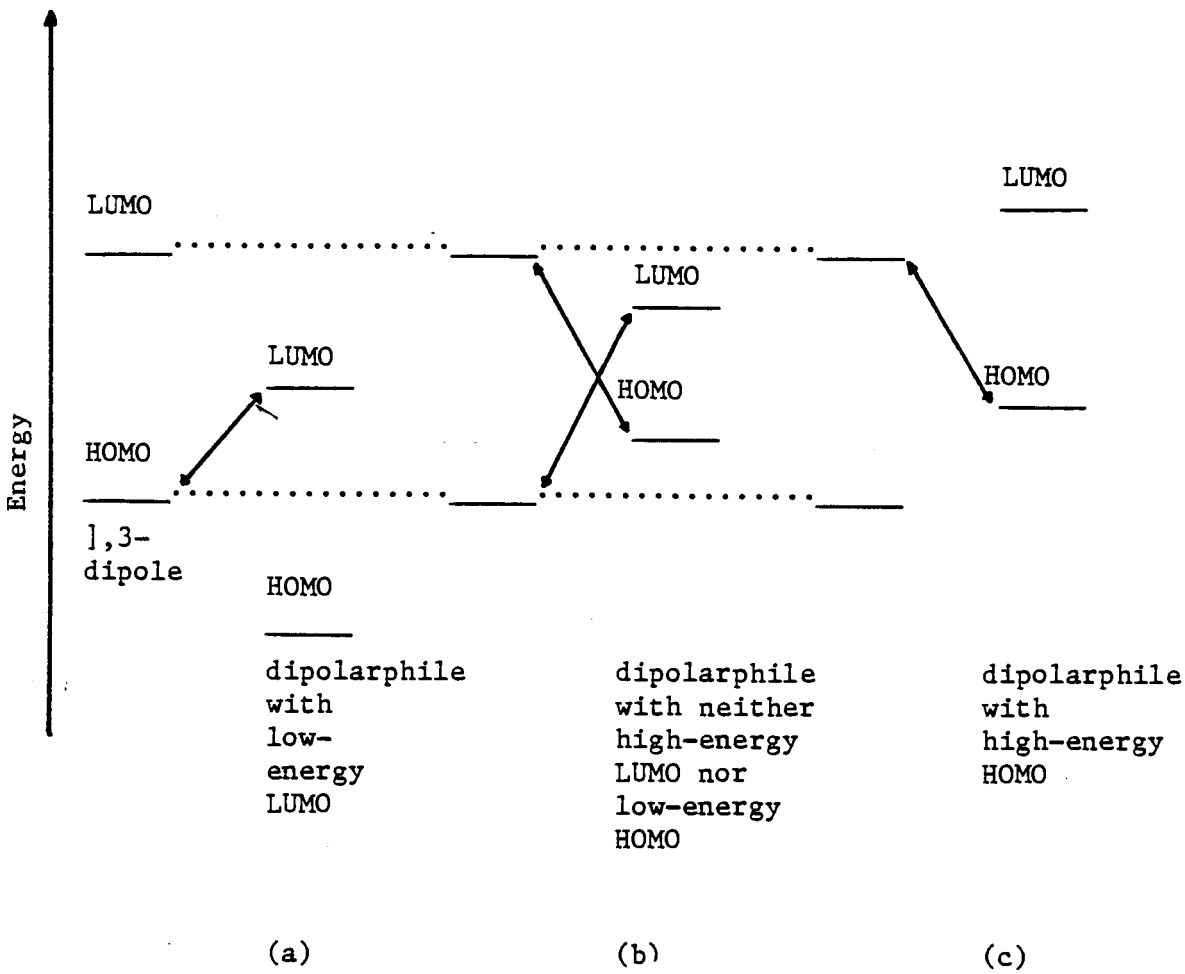

Figure 3-2. Frontier orbital interactions.

Table-8. Frontier Orbitals Coefficients and Energies for Olefins[43,48] and Nitrones[44,45,49].

Olefins	Energies(eV)		C_1	C_2	C_3	C_4
I	LU	+ 3.84	+0.659	-0.537	-0.298	+0.436
	HO	-13.95	-0.606	-0.497	+0.328	+0.528
II	LU	+ 3.56	+0.438	-0.307	-0.462	
	HO	-11.80	-0.460	-0.312	+0.457	
III	LU	+ 3.07	+0.601	-0.391	-0.501	+0.436
	HO	-12.89	-0.290	-0.216	+0.250	+0.736
IV	LU	+ 2.23	+0.566	-0.566	+0.207	-0.370
	HO	-13.00	-0.510	-0.510	+0.227	+0.434
V	LU	+ 1.50	+0.472	-0.472	+0.346	-0.360
	HO	-12.70	-0.303	-0.303	+0.172	+0.552
VI	LU	+ 3.60	+0.488	-0.488	+0.341	-0.381
	HO	-13.60	-0.250	-0.250	+0.148	+0.532
VII[a]	LU	- 0.50	+0.980	-1.030	+0.320	
	HO	- 9.70	+1.110	+0.050	-1.060	
VIII	LU	+ 0.30				
	HO	- 8.70				
IX	LU	- 0.40				
	HO	- 8.00				

a: The values of the coefficients are $(C\beta)^2/15$

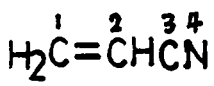
I

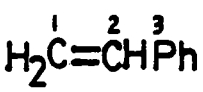
II

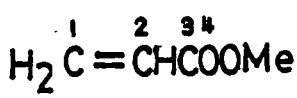
III

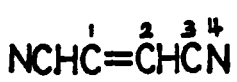
IV

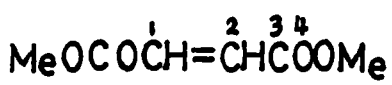
V

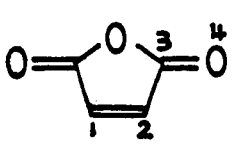
VI

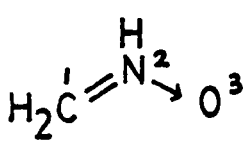
VII

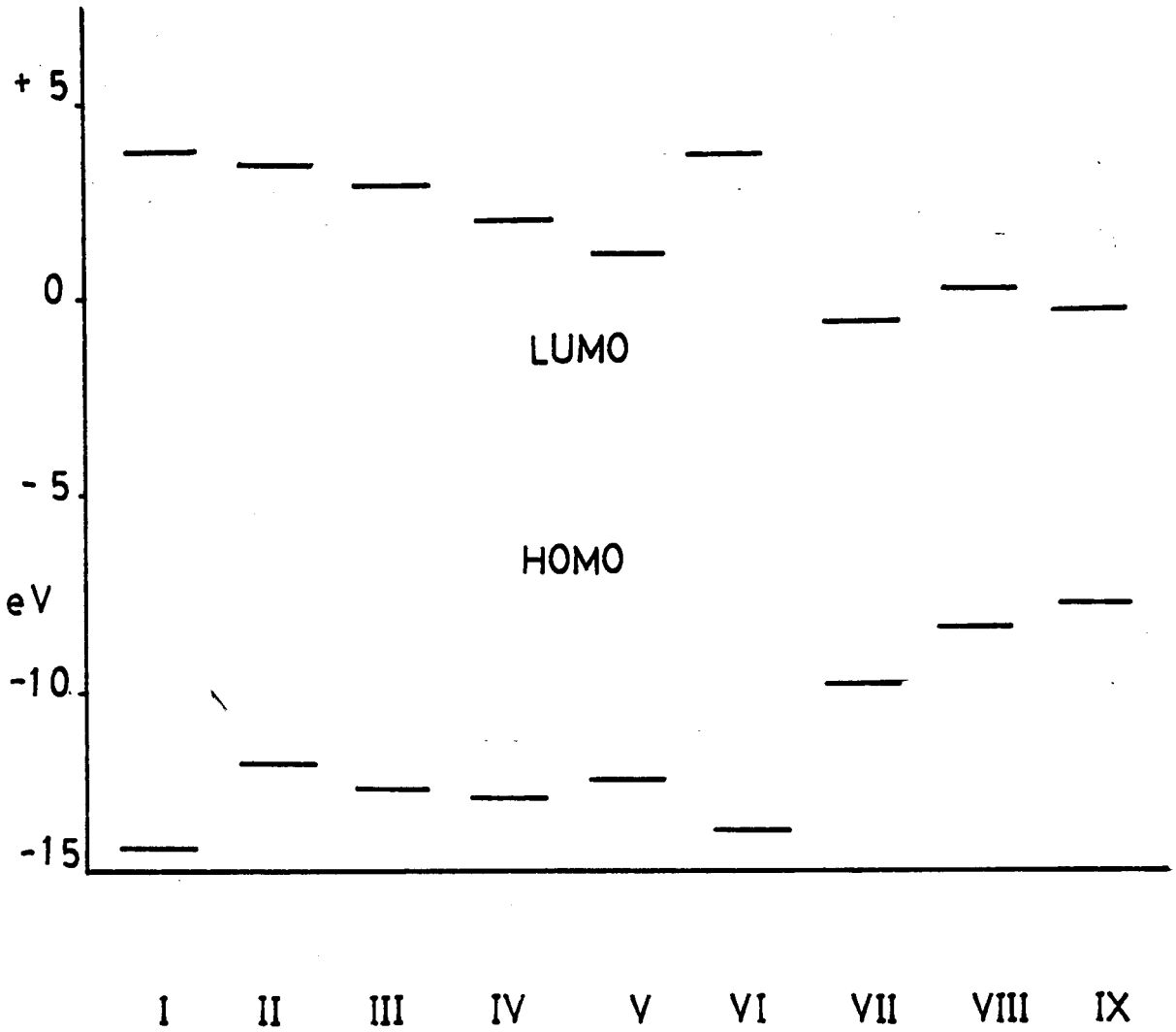

Figure 3-3. HOMO and LUMO Energy Levels of Olefins and Nitrones

The componds I to VII are the same as in Table-8.

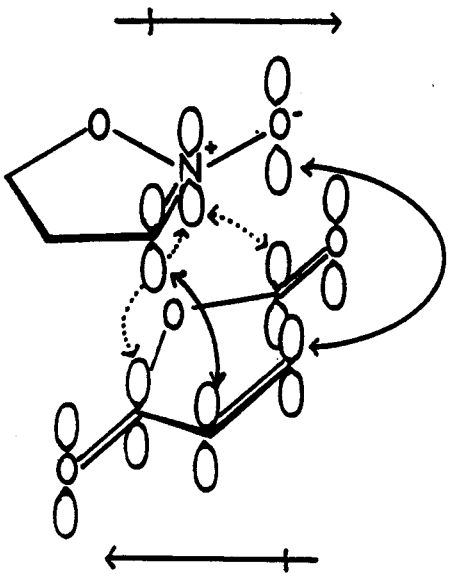

Figure 3 - 4 Secondary overlap of the frontier orbitals of N-oxide 1 to maleic anhydride from endo approach.

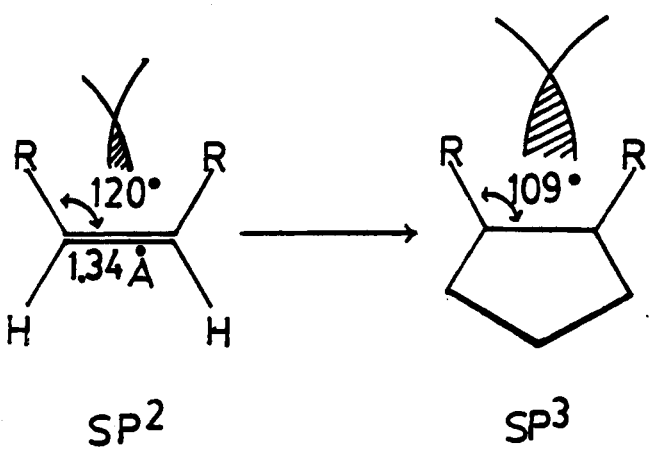

Figure 3 - 5

The fact that the cycloadditions of N-oxide 1 to trans-olefins give predominantly TX adducts might be alternatively explained by the favorable overlap of the frontier orbitals in the transition state. For instance, there is a control from secondary orbital interaction in the reaction involving HOMO(dipole)-LUMO(olefin); as shown in Figure 3-6a[52] , such a control exists in the TX approach but not in the TN approach(Figure 3-6b) [53]. It whould be noted that in the reaction involving LUMO(dipole)-HOMO(olefin) such difference no longer exists.

The regiochemistry of the cycloaddition of 1 to mono-substituted olefins might also be considered in terms of this theory. Houk reported that the regioselectivity is determined by the coefficients on the reaction centers of the two reactants[54]. Assuming that the C-N-O moiety of N-oxide 1 possesses the same calculated HOMO-LUMO energies and coefficients of the parent $CH_2=N^+H-O^-$ system[44,45,49](see Figure 3-7), the large coefficient of C-3 and the small coefficient of O match with the corresponding ends of the olefin.

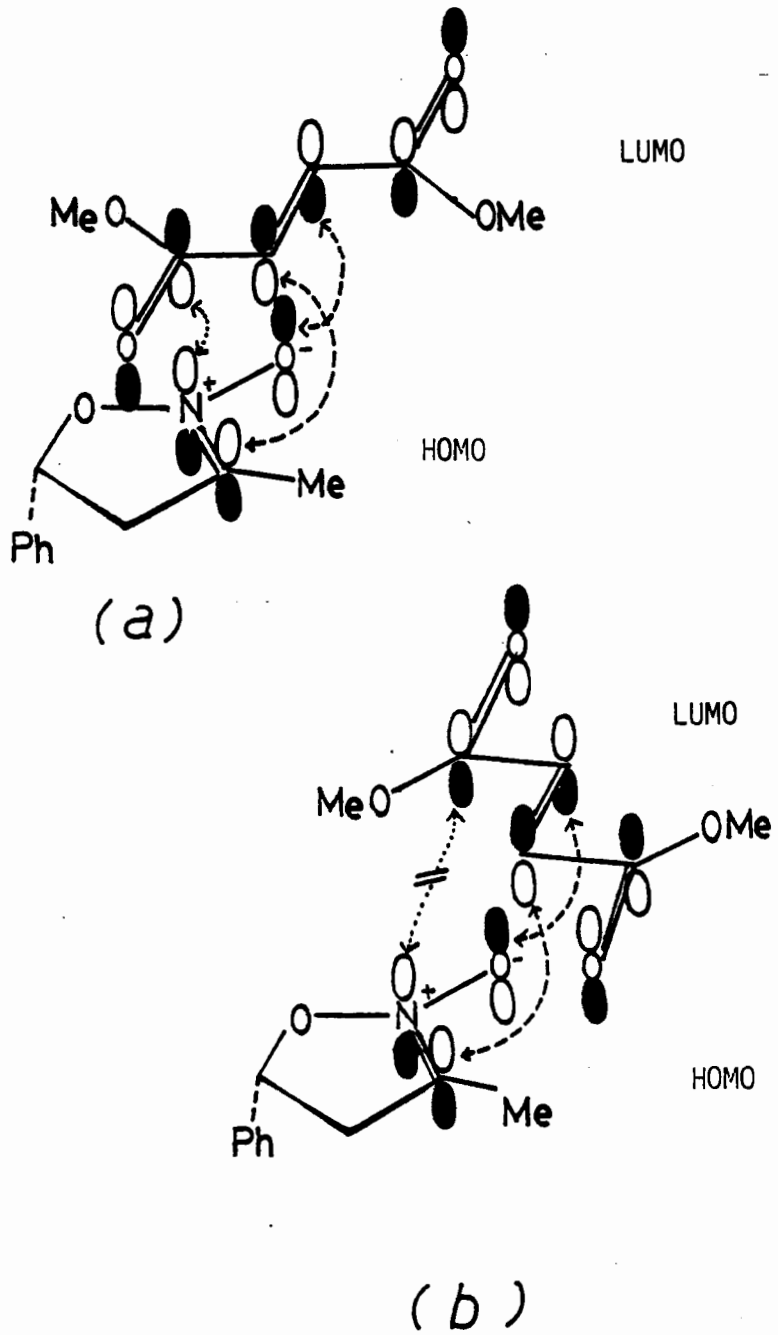

Figure 3 -6. Secondary orbital interaction(.....) of the cycloaddition of 1 to dimethyl fumarate in (a)TX and (b) TN approaches.

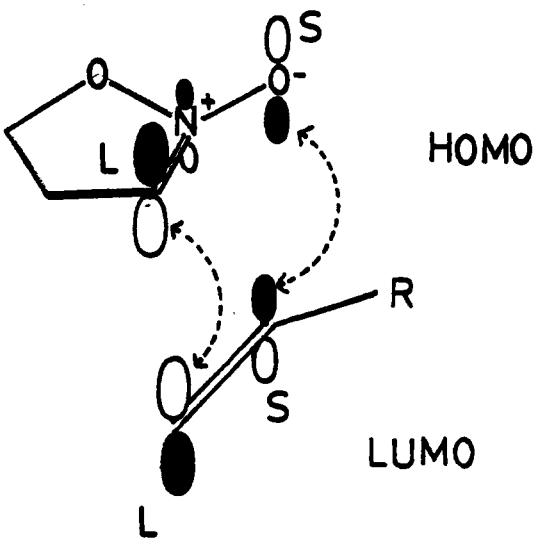

L: large orbital coefficient; S: small orbital coefficient

R = CN
Ph
COOMe

Figure 3 - 7. Frontier orbital coefficients of the 1,3-dipolar cycloaddition.

4. Conformational Properties

In the top-addition products, H_c consistently resonates at a higher field than H_b; the opposite situation is observed in the bottom-addition products. These chemical shift differences may be explained by the shielding effects of the phenyl ring in its favorable orientation. In Figure 3-8a, the H_b is in a more deshielded position than that of H_c; and in Figure 3-8b, they are in the reverse position. Also, in most of the cases, the signal of H_a in the endo position(Figure 3-8a) is located at a lower field than the signal from the exo position(Figure 3-8b). The dependence of the chemical shift of the H_a on orientations is obviously connected with the anisotropic effects of the O-N-O moiety, methyl group, and substituents at 6- and 7-positions. The chemical shift of the 5-methyl group is slightly affected by the 5-phenyl, 6- and 7- substituents in all the cases except for adducts 11.

Applying the Karplus' plot of dihedral angles vs coupling constants as well as NOE results of vicinal protons in the cycloadducts, we can approximate the dihedral angles of H_a-H_b and H_a-H_c. The Newman projections in Figure 3-8 provide the general idea of dihedral angles. The J_{ac} is larger than the J_{ab} in the top-addition adduct while the reverse is true in the bottom-addition adduct in most of the cases except for 9TX, 11TN and 11BN. Merely using coupling constants to determine the

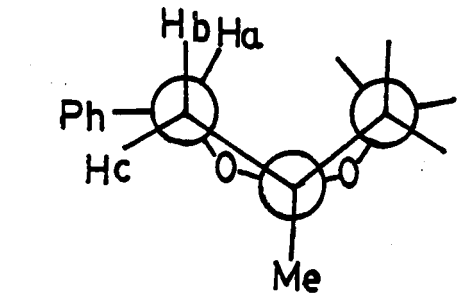

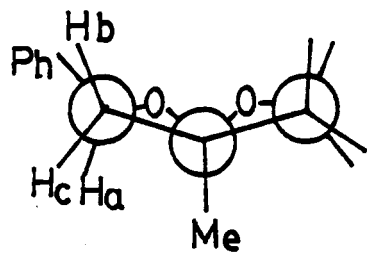

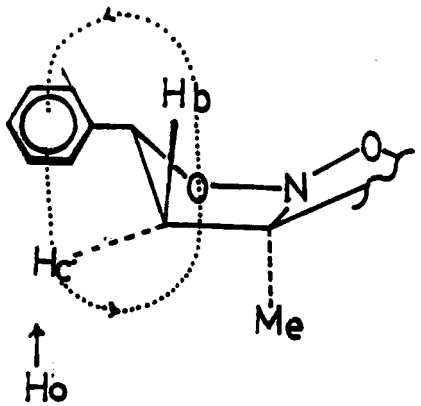

a. top-addition adduct

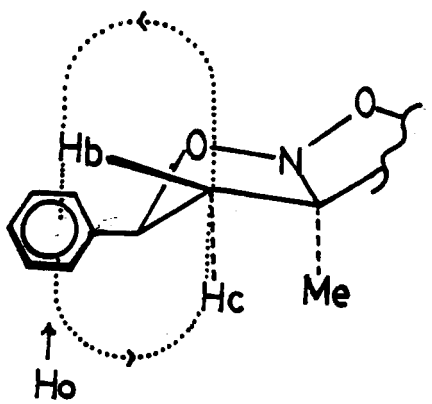

b. bottom-addition adduct

Figure 3-8. Newman projections of 1-aza-2,8-dioxabicyclo [3.3.0]-octanes and the shielding effect of 3-phenyl group.

structures of this type of cycloadduct is inadequate because of the exceptions. In the present cases, NOE results are used concurrently to ascertain the structures.

5. High Pressure Reaction

The cycloaddition carried out under high pressure leads to improvements in rate[55], yield[56], and stereoselectivity [57]. The 1,3-dipolar cycloadditions of nitrone with ethyl vinyl ether and vinylidene carbonate under 1, 2, and 4K bar have been reported by DeShong[58]. He concluded that (1) a high pressure can effect [3 + 2] cycloadditions at room temperature giving yields which generally exceed those at a higher temperature and the normal pressure, and (2) the stereoselectivity of the cycloaddition is altered by the shift from normal to high-pressure conditions. As shown in Table-3, the high pressure cycloadditions of N-oxide 1 with di-substituted olefins are more stereoselective than those at one bar. The stereoselectivity is improved except in the cycloaddition with methyl acrylate.

Under high pressure, the two reactants are packed more tightly than under low pressure. The less hindered pathway, i.e. the top-exo approach, should be preferred, and this is observed in the cycloadditions to dimethyl fumarate and fumaronitrile in which the bottom approaches are reduced. As the

stereoselectivity in the cycloaddition with maleic anhydride under normal pressure is fairly high, the increase of the top-endo adduct is slight under the high pressure conditions.

6. The Formation Constants of the Ground State Complex

Maleic anhydride forms an observable ground state complex with N-oxide 1 even at lower concentrations, and shows addition reactivity. In contrast, the ground state complex of vinyl acetate was not observed and shows no addition reactivity. These observations might suggest a relationship between ground state complex formation and cycloaddition. Complex formation is not observed between N-oxide 1 and dimethyl fumarate or dimethyl maleate while both show cycloaddition reactivity. It is possible that the formation constants in these cases are very small or the molar absorptivities of the complexes are not very different from either the olefins or N-oxide 1.

Equation {2} was applied to calculate for both K value of fumaronitrile and trans-stilbene, because the spectroscopic conditions are similar to the determination of the equilibrium constant of proton-donor-acceptor complex of ethylene trithiocarbonate and thiophenols[59]. The trans-stilbene N-oxide 1 ground state complex is easy to observe because of its large K value, although the difference in molar absorptivities at 294 nm

between trans-stilbene(≃34600) and the complex(≃35090) is not significant. The fumaronitrile N-oxide 1 ground state complex is observed because of the large difference between the molar absorptivities at 267 nm of N-oxide 1 (≃170) and the complex (≃1290), although the K is not large.

Because of the low absorptivities of maleic anhydride (≃16) and N-oxide 1(<3) at 300 nm, equation {1} was utilized in the determination of the K for complex formation. We can assume that the absorbance due to the N-oxide 1 is negligible at the concentration used. Since the molar absorptivity of the complex(≃140) is large, its formation can be observed at the concentrations of maleic anhydride used(0.0048-0.02 M).

The failure of trans-stilbene to give a cycloadduct in spite of efficient ground state complex-formation is puzzling; it is possible that the stereochemistry of the ground state complex is not favorable for cycloaddition. In other words, the charge transfer does not occur on the ethylene moiety of stilbene.

In summary, it may be suggested that the ground state complex is on the pathway to the final cycloaddition product[60] in some cases.

CHAPTER 4

EXPERIMENTAL

1. General Techniques

Unless specified otherwise, the following conditions prevail in the experiments.

1. Infrared spectra were taken on a Perkin-Elmer 559B spectrophotometer in liquid film or nujol mull using NaCl windows.
2. Ultraviolet spectra were recorded on a Varian Cary 210 or Unicam SP-8000 spectrophotometer; spectral bands are reported as λ max nm.
3. Nuclear magnetic resonance spectra were taken on a Bruker WM -400 spectrometer in deuterochloroform; chemical shifts are reported in δ(ppm) units, coupling constants(J) in hertz(Hz), the coupling patterns as s(singlet), d(doublet), t(triplet), q(quartet), m(multiplet), dd(double-doublet) and the number of protons by H.
4. Mass spectra were obtained on a Hewlett Packard 5985 spectrometer with the ion voltage at 70eV by Mr.G.Owen. The significant peaks are reported as relative abundance m/e.
5. Melting points were determined by a Fisher Johns hot stage apparatus and were not corrected.

6. Separations by high performance liquid chromatography(HPLC) were performed using a Waters 440 uv detector and a 660 solvent programmer. HPLC was carried on a Waters u-Porasil P/N 27477 S/N analytical column and a Whatman Partisil M90 10/50 preparative column.
7. Separations by flash column chromatography were performed using Merck silica gel 60(230-400 mesh). Thin layer chromatography (TLC) was performed on silica gel plates (Merck silica gel 60 F_{254},0.2mm).
8. The percentage of conversion of starting material and the ratio of isomers were estimated from NMR analyses.
9. Elemental analyses were performed by Mr.M.K.Yang, Department of Biological Sciences and are reported in TABLE-15.

2. Chemicals

Reagent grade solvents were distilled before use. Reagent grade acetonitrile(Caledon) was refluxed with phosphorus pentoxide and distilled. Methyl acrylate(Matheson), acrylonitrile(Aldrich), and vinyl acetate(Fisher) were distilled before use. Styrene (Eastman) and dimethyl maleate were distilled under reduced pressure. Fumaronitrile(Aldrich) was recrystallized from ether. Maleic anhydride (Fisher) was

recrystallized from CH_2Cl_2. Dimethyl fumarate (Aldrich,97%) and trans-stilbene(Matheson) were used as supplied.

3. The General Procedures of Cycloadditions

A solution of N-oxide 1(0.5-3.5mmol) and olefin(1-20mmol) in acetonitrile(15-50ml) were placed in a three-necked round bottom flask or a Schlenk tube and heated in an oil bath under purified nitrogen(Fieser's solution) with magnetic stirring. The reaction was monitored by TLC until the 95-100% disappearance of the TLC spot of 1. The reaction mixture was evaporated under vacuum and the residue was evacuated at 1mm Hg pressure. The crude products were examined by NMR spectroscopy and HPLC analyses. Generally, the crude products were separated by flash chromatography or preparative HPLC using isopropanol-hexane as eluent. The spectral data of cycloadducts are listed in Table-9 to 14 and the elemental analyses are listed in Table-15.

4. The Preparation of N-oxide 1

A solution of 1-phenyl-1-dimethylsulfoniumbromide-2-bromoethane(9.0g,28mmol)

and nitroethane(4ml,56mmol) in 10% aqueous K_2CO_3 solution (150ml) was kept at 50° for 2 hours with magnetic stirring. The yellow oil gradually formed, suspended in the solution. The oil was extracted with ether(50mlx5) and washed with 10% aqueous K_2CO_3 solution and with water. The ether solution was dried over $MgSO_4$ for 1 day and was flash evaporated. A crude yellowish solid product of N-oxide 1 was obtained in a 85% yield (3.98g) and was recrystallized from ether(150ml)-pentane (200ml) twice and washed with cold ether to give colorless crystals. After drying the crystals under reduced pressure by an oil pump for 2 hours, pure 1 was obtained: m.p.73°C; IR(nujol) 1640 cm^{-1}(C=N); ^1H NMR($CDCl_3$) 2.05(t,3H), 3.05 (ddq,1H,J=18.5;8.5), 3.50(ddq,1H, J=18.5;10.0), 5.70(dd,1H,J=10.0; 8.5), 7.30(m,5H); MS(EI mode), m/e 41, 51, 77, 91, 105(base), 129, 130, 131; MS(CI mode) M+1 m/e 178; UV(CH_2Cl_2): ϵ_{267}=173; ^{13}C NMR($CDCl_3$,decoupled): 139.02, 128.92, 128.70, 125.55, 111.90(quaternary), 75.33(methyne), 42.25 (methylene),11.75ppm(methyl); ^{13}C NMR(CCl_4):140.3(s), 129.0(d),128.6(d),125.8(d),109.1(s),74.9(d),42.7(t),12.2ppm(q).

Anal.Calcd. for $C_{10}H_{11}NO_2$: C,67.78; H,6.26;N,7.90. Found: C,67.59; H,6.11; N,7.91.

5. Cycloadditions of N-oxide 1 to Olefins

5a. Cycloaddition of N-oxide 1 to Methyl Acrylate.

A solution of 1(200mg,1.1mmol) and methyl acrylate (2ml,22mmol) in acetonitrile(30ml) was kept at 50°C for 93 hours at which time 1 had been consumed completely. The yellow residue (≃302mg) showed four HPLC peaks(0.5% isopropanol-hexane at 2 ml/min.) at 15.46,16.42,24.17, and 25.43 minutes for cycloadducts 6BN, 6TN,6BX, and 6TX, respectively, in a ratio of 8:20:18:44. The NMR spectrum showed four methyl signals in the ratio of 12:19:19:50 corresponding to cycloadducts 6BN, 6BX, 6TN, and 6TX, and no olefinic- methyl signal corresponding to 1. 219/6mg of crude product was purified by flash chromatography (30% acetone/hexane) yielded three fractions. The first fraction was a colorless solid(20mg, 9% on the basis of N-oxide 1) containing 6TX, 6BX, 6TN and 6BN in the ratio of 4:10:79:7 by NMR analysis and of 5:7:74:9 by HPLC analysis which showed no additional peak. The second fraction was a colorless oil (105mg, 48% on the basis of1) containing 6TX, 6BX, 6TN and 6BN in the ratio of 49:18:21:12 by NMR analysis; HPLC showed four closely placed peaks but no other peaks. The third fraction was a colorless oil (54mg, 25% on the basis of 1) containing 6TX, 6BX and 6TN in the ratio of 79:16:5 by NMR analysis; HPLC showed two peaks in the ratio of 86:7 (6TX:6BX) and one peak which could not be integrated corresponding to 6TN and no other peaks. Preparative HPLC(2.5% isopropanol-hexane at 5ml/min.) gave fractions that were crystallized from acetone-hexane to give four cycloadducts 6BN (oil, contaminated by about 30% of 6TN), 6TN (colorless solid, m.p.71-74°C), 6BX (colorless needles, m.p.

92-94°C), and 6TX (colorless solid, m.p. 78-80°C).

5b. Cycloaddition of N-oxide 1 with Styrene

A solution of 1(208mg, 1.2mmol) and styrene(1ml, 9.6mmol) in acetonitrile(30ml) was kept at 50°C for 5 days at which time 1 was not observed from TLC analysis. The yellow brown residue showed two HPLC peaks(5% isopropanol-hexane at 5ml/min., preparative column) at 7.87and 9.50 minutes for cycloadducts 7TX and 7TN respectivily, in a ratio of 31:24. The NMR spectrum showed two methyl signals in the ratio of 54:46 corresponding to cycloadducts 7TX and 7TN, and a small signal at 2.01 ppm corresponding to the olefinic methyl of 1. Comparing the integrations of the methyl signals of cycloadducts and the olefinic-methyl signal, the calculated conversion of 1 is 95%. 20mg of the crude product was taken for preparative HPLC(same conditions as above) gave fractions that were crystallized from the eluent when the amount of eluent was reduced by evaporation to give cycloadducts 7TX(3mg , colorless needles, m.p.140-143°C) and 7TN(1mg, colorless fine needles, m.p.121-123°C).

5c. Cycloaddition of N-oxide 1 with Acrylonitrile

A solution of 1(150mg,0.85mmol) and acrylonitrile(0.3ml, 5.7mmol) in acetonitrile(25ml) was heated at 95°C for 5 days at which time 1 had been consumed completely. The yellow oily

residue showed three HPLC peaks(5% isopropanol-hexane at 2 ml/min.) at 20.78, 22.10, and 35.50 minutes for cycloadducts 8TN (or 8BX or 8BN), 8TX, 8BX(or 8BN or 8TN), and 8BN(or TN or BX), respectively, in a ratio of 20:53:32(where the third peak includes two products). The NMR spectrum showed four methyl signals in the ratio of 9:25:10:5, corresponding to cycloadducts 8TN(or BX or BN),8TX,8BX(or BN or TN), and 8BN (or TN or BX), and no olefinic-methyl signal corresponding to 1. Preparative HPLC(5% isopropanol-hexane at 5ml/min.) gave 8TX from the second fraction as colorless crystals recrystallized from acetone-hexane, m.p.98-99°C, and two more unidentified fractions. The first fraction(colorless oil) which could be 8TN (or BX or BN) was contaminated with 8TX and the third fraction was a mixture of the two cycloadducts(which could be two among the three cycloadducts 8TN,8BX, and 8BN).

5d. Cycloaddtion of N-oxide 1 with Dimethyl Fumarate

A solution of 1(100mg, 0.56mmol) and dimethyl fumarate (100mg, 0.69mmol) in acetonitrile(25ml) was kept at 85°C for 18 days until 1 was consumed completely. The brown oily residue showed three HPLC peaks(2.5% isopropanol-hexane at 5ml/min., preparative column) at 10.30, 15.93, and 17.10 minutes for cycloadducts 9TN, 9BN, and 9TX respectively, in a ratio of 89:49:92. The NMR spectrum showed three Hd signals in the ratio of 31:19:50 corresponding to cycloadducts 9TN,9BN and 9TX

respectively. Preparative HPLC(same conditions as above) gave fractions that were crystallized from acetone-hexane or from reducing the amount of eluent to give three cycloadducts 9TN (colorless crystals, m.p.110-112°C), 9BN(colorless crystals) , 9TX(colorless hexagonal crystals, m.p.96-97.5°C).

5e. Cycloaddition of N-oxide 1 with Fumaronitrile

A solution of 1(300mg, 1.70mmol) and fumaronitrile(200mg, 2.56mmol) in acetonitrile(30ml) was refluxed for 7 days until 1 was consumed completely. The brown residue showed four HPLC peaks (10% isopropanol-hexane at 5ml/min., preparative column) at 13.76, 15.72, 17.61 and 18.62 minutes for cycloadducts 10TX, 10TN, 10BN, 10BX respectively, in a ratio of 13:5:1:8. The NMR spectrum showed four methyl signals in the ratio of 71:14:5:10 corresponding to cycloadducts 10TX, 10TN,10BN, and 10BX. The ratio of the cycloadducts showed on the HPLC is different from that showed on the NMR spectrum might be caused from the overlap of the peaks and impurities. The residue was dissolved in hot ether and cooled to give a white precipitate which was crystallized twice from same solvent to give 10TX(colorless crystals, m.p.119-120°C). The mother liquors were concentrated under reduced pressure and chromatographed by HPLC to give 10TN (colorless solid, contaminated with 10TX and 10BN) and 10BX(white solid,contaminated with the other three isomers) The HPLC peak corresponding to 10BN was located close to those of 10TN

and 10BX and was obtained as a mixture with other products.

5f. Cycloaddition of N-oxide 1 with Dimethyl Maleate

A solution of 1(325mg,2mmol) and dimethyl maleate(1ml, 8mmol) in acetonitrile(30ml) was heated at 95°C for 42 days and left at 22°C for another 60 days until the spots of 1 disappeared from the TLC plate. The brown residue showed one tailing spot on TLC (Rf=0.42, eluent:2% isopropanol-CH_2Cl_2). The NMR showed two methyl signals in the ratio of 13:7 corresponding to the cycloadducts 12TX and 12BX. The residue was flash chromatographed to give 12BX(white solid, contaminated with 12TX) and 12TX(small needles from acetone- hexane; m.p.135-136°C). The NMR spectrum also showed a small amount of unreacted 1, and the conversion as 94%. This was calculated from the comparison of the integration of the olefinic-methyl signal and methyl signals of the cycloadducts.

5g. Cycloaddition of N-oxide 1 with Maleic Anhydride

A solution of 1(600mg, 3.4mmol) and maleic anhydride(250mg, 2.5mmol) in acetonitrile(17ml) was refluxed for 8 hours until the maleic anhydride was completely consumed. The brown residue could not give accurate HPLC data because of serious tailing from every peak. The NMR spectrum showed four methyl signals(1.49, 1.54, 1.53, 1.57ppm) in the ratio of 78:15:5:2

corresponding to cycloadducts 11TN, 11TX(or BX), 11BX(or TX) and 11BN, and no olefinic-proton signals(7.10ppm) corresponding to maleic anhydride. The residue was recrystallized from CH_2Cl_2-hexane twice to give 11TN(colorless crystals, decomposed at 160°C) which contained 11BN in the ratio of 17:3. The mother liquors were concentrated under reduced pressure and dried over an oil pump for 2 hours. This residue from the mother liquors decomposed during an attempt at flash chromatography (30% acetone-hexane). Brown oily residues were obtained from the two fractions. They gave broad undistinguishable NMR signals. No ABX pattern protons of cycloadduct signals were observed.

5h. Cycloaddition of N-oxide 1 with Vinyl Acetate

A solution of 1(200mg, 1.1mmol) and vinyl acetate(.2ml, 2.3mmol) in acetonitrile(50ml) was kept at 95°C for 9 days. The brown solution gave two HPLC peaks corresponding to the two starting materials . And the brown residue obtained from the brown solution showed the same NMR and IR spectra as those of N-oxide 1.

5i. Cycloaddition of N-oxide 1 with trans-Stilbene

A solution of 1(90mg, 0.5mmol) and trans-stilbene (87mg,0.5mmol) in acetonitrile (20ml) was refluxed for 90 hours. HPLC showed no cycloadduct peak for the solution. The NMR

spectrum from the recovered solid was identical with that of 1 and trans-stilbene.

5j. Cycloaddition of N-oxide 1 to Vinyl Methyl Ketone

A solution of 1(174mg,0.98mmol) and vinyl methyl ketone (90ul,1.1mmol) in acetonitrile(6ml) was heated at 45°C for 6 days when 1 had disappeared from TLC analysis. NMR(60MHz) showed two signals at 1.50 and 1.55ppm corresponding to the methyl group of the cycloadducts. A impure white crystal (m.p.81-85°C) with red spots was obtained by recrystallization from ethylacetate-hexane(3:7) showed NMR: 1.50 (s,3H), 2.17 (dd,1H), 2.37 (s,3H), 2.40 (dd, 1H), 2.63(dd,2H), 4.63(dd,1H), 5.58(dd,1H), and 7.40(m,5H). IR (nujol): 1720(C=O), 1490, 1450, 1380, 1350, 1280, 1230 and 1080 cm^{-1}.

5k. Reaction of N-oxide 1 with Nitrosobenzene

A solution of 1(89mg,0.5mmol) and nitrosobenzene(54mg, 0.51mmol, recrystallized from acetone) in acetone(20ml) was stirred at room temperature(22°C) under nitrogen atmosphere. During 25 minutes, the original blue color turned gradually to green, and after 45 minutes had become yellow. The yellow solution(2ml) was flash evaporated and dried under reduced pressure for NMR and ESR measurements. The remaining solution turned red after stirring for another 3 hours. The red solution

was evaporated under reduced pressure to give a deep red oil. The ^1H NMR spectrum of the red solution gave weak signals characteristic of 1 and a new unknown product. Their the ratio was 1:23 on the basis of the integrations of the olefinic-methyl signal(2.01ppm) of 1 and the methyl signal (2.19ppm) of the new product. The ratio of 1 to the new product for the yellow solution was 4:7. Both yellow and red solutions showed easily distinguishable NMR spectra. The signals of the new product are located at (in $CDCl_3$) 2.19ppm(s,3H), 2.82 (dd,1H), 2.09(dd,1H), 5.16(dd,1H), and 7.21-7.55(m,10H) where the three protons are in an ABX pattern. The red oil gave tailing spots on the TLC plate. IR(neat) of the red oil showed: 3360 cm^{-1} (broad), 3060(m), 3020(m), 1710(s), 1650(m), 1590(m), 1490(m), 1450(m), 1360(broad,s), 1310(broad,s), 1250(broad,s), 1230(broad, s), 1160(m), 1110(m), 1060(s), 920(w), 870(m), 760(s), 705(s). MS by EI mode gave m/e at 50, 51, 77(base), 78, 79, 91, 103, 104, 105, 106, 107, 131, 145, 146, and 164. MS by CI mode(iso-butane) gave m/e at 107 and 147, and no peak at 285. ^{13}C NMR ($CDCl_3$) gave 209.0, 142.78, 129.65, 128.96, 128.91, 128.71, 128.52, 128.24, 127.67, 125.61, 125.54, 69.89, 51.94, and 30.68ppm. ESR signals of the yellow solution(Figure 4-1) showed a splitting pattern similar to that of the red solution(Figure 4-2) but noisy. The ESR signal (Figure 4-3)of the red oil was recorded after the oil had been frozen for 24 days. Figure 4-4 was taken after being exposed to light for 24 days at room temperature for the same

Figure 4-1. ESR signals of the yellow solution.

solvent:CH_2Cl_2

microwave power: 20mW

Figure 4-2. ESR signals of the red oil

solvent:CH_2Cl_2

g=2.0078

a=10.25G

standard: Varian Strong Pitch Sample

(g=2.0026)

microwave power: 20mW

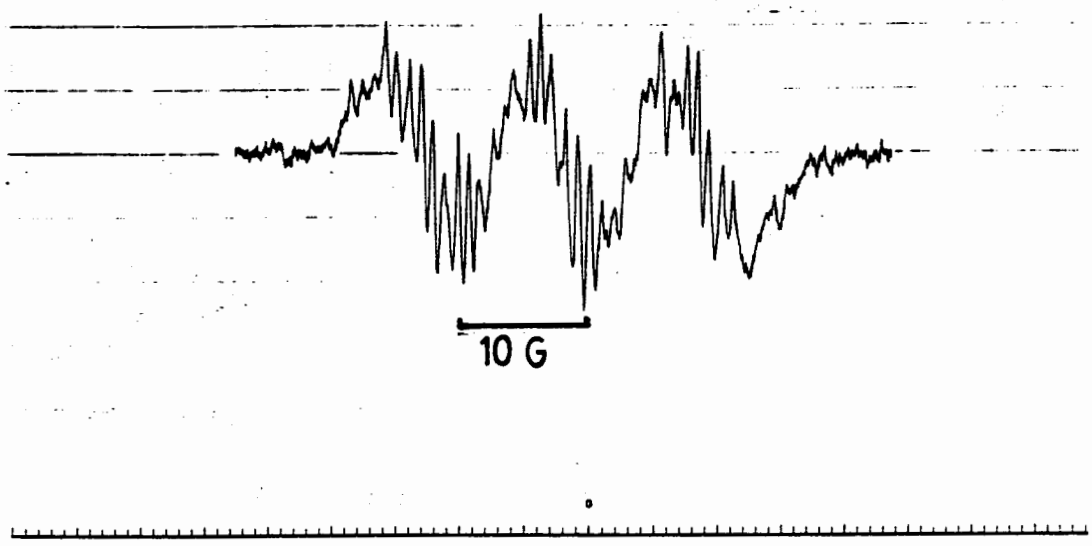

Figure 4-1

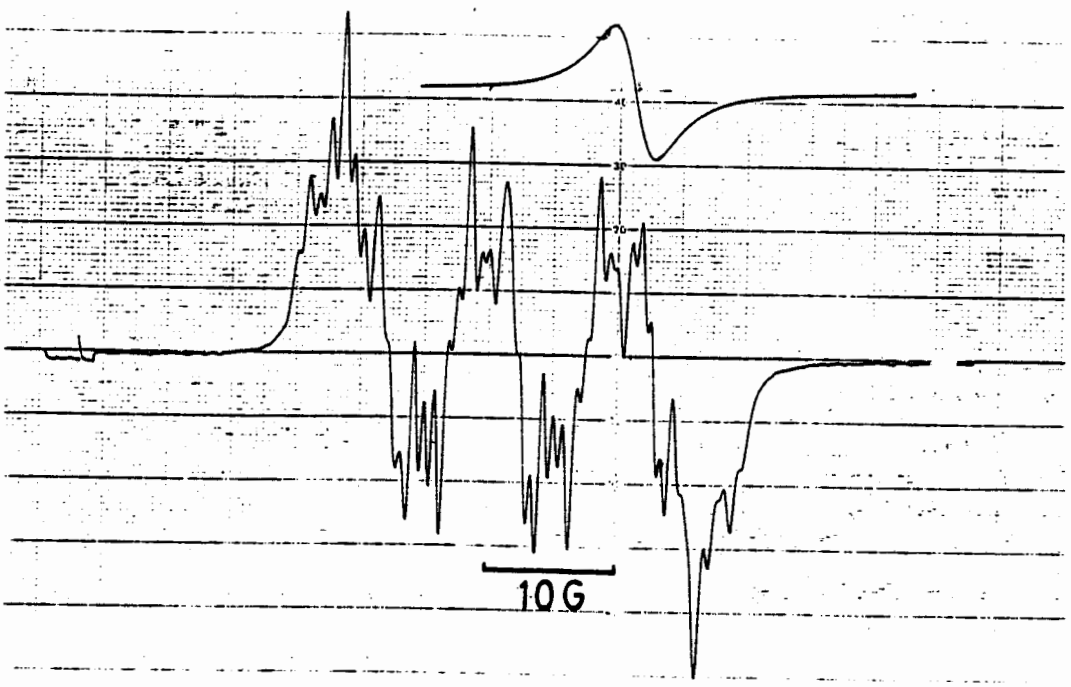

Figure 4-2

Figure 4-3. ESR signals of the red oil after being frozen for 24 days.
solvent: same as above
microwave power: 5mW

Figure 4-4. ESR signals of the red oil after begin exposed to light for 24 days.
solvent: same as above
Microwave power: 40mW

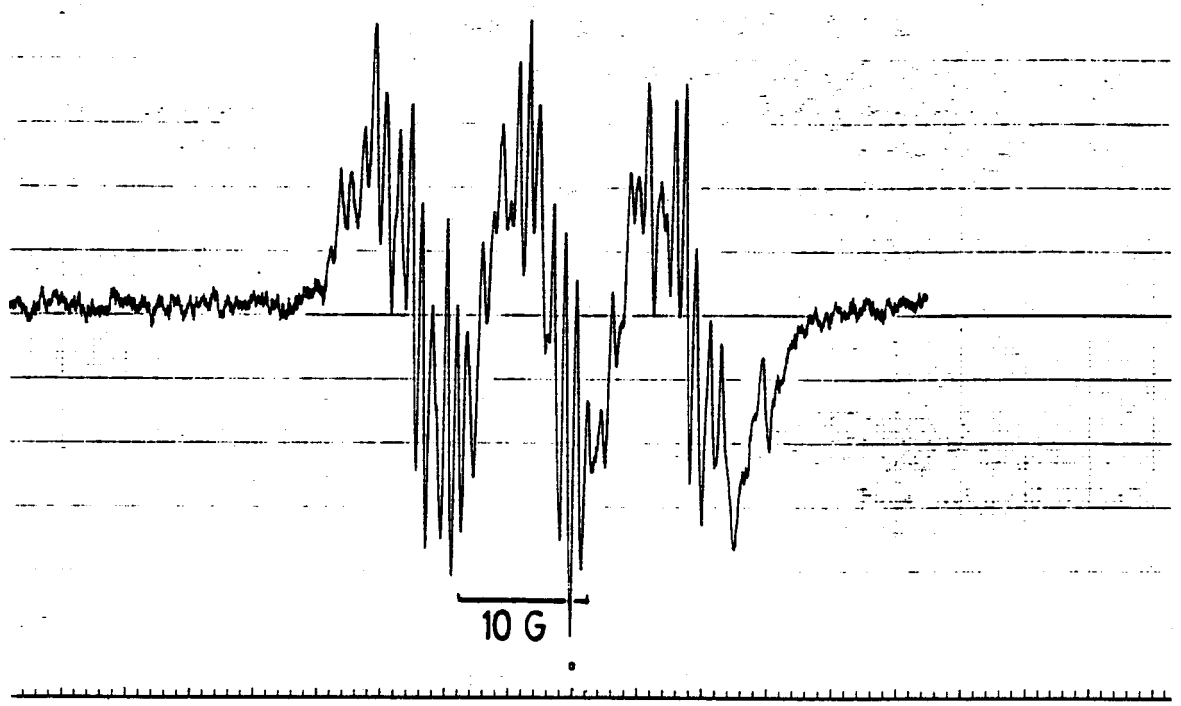

Figure 4-3

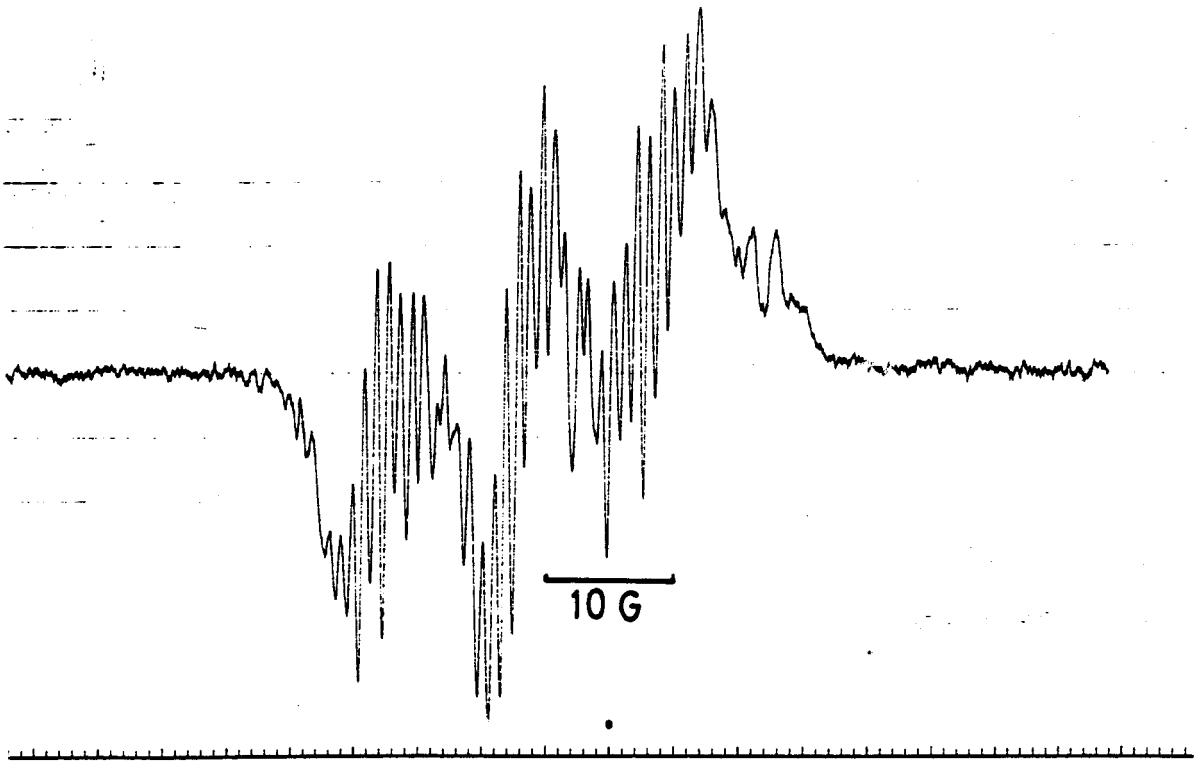

Figure 4-4

sample as in Figure 4-2. The g and a values obtained from Figure 4-2 are 2.0078 and 10.25G respectively.

6. Test for kinetic vs. thermodynamic control

A solution of 6BX(3mg) in acetonitrile(1ml) was kept at 50°C for 135 hours. After flash evaporation, a white solid (2.7mg) was obtained. The NMR spectrum showed only signals corresponding to 6BX. No other cycloadduct was found.

A solution of a 75:25 mixture of cycloadducts 8TX:8TN (10.5 mg, white solid) in acetonitrile(1ml) was kept at 95°C for 120 hours. The color of the solution turned light yellow after heating for two days. A white solid (9.9 mg, contaminated with a yellow oil) was obtained after flash evaporation. The NMR spectrum of the crude material showed the signals corresponding to the starting materials 8TX and 8TN in 3:1 ratio. No signals corresponding to other cycloadducts were found.

7. Cycloadditions under High Pressure

The high pressure cycloadditions were carried out under the pressure of 1.38 to 2.07KBar. The pressure reactor(Figure.4-5) is connected with an hand-operated oil pump(Pressure Products Industries, Div.of the Durion CO., INC., Hatboro, PA., Mod.OH-102-60W).

Solutions containing 1(.1-.2mmol) and olefins(.2-.4mmol) in acetonitrile(.35ml) were placed in a reaction vessel. The pressure was increased through paraffin oil medium at room temperature (22 °C). At intervals, the pressure was released and the reactions were monitored by HPLC. The samples were evaporated and dried over reduced pressure for 2-3 hours and examined with NMR when the N-oxide 1 peak was not observed from HPLC analyses.

7a. Reaction of N-oxide 1 with Dimethyl Fumarate.

A solution of 1(19mg,0.11mmol) and dimethyl fumarate (38mg,0.26mmol) in acetonitrile(.35ml) was placed under 2.07KBar at room temperature and monitored by HPLC every 24 hours. After 240 hours, the peak corresponding to 1 had disappeared. The NMR spectrum of the residue showed the Hd signals corresponding to cycloadducts 9TX, 9TN, and 9BN in the ratio: 63:25:12.

7b. Reaction of N-oxide 1 with fumaronitrile.

A solution of 1(16mg,0.09mmol) and fumaronitrile(20mg, 2.56mmol) was placed under 1.38KBar for 54 hours until 1 was consumed completely. The reaction was monitored by HPLC every 6 hours. The NMR spectrum of the residue showed the methyl signals corresponding to 10TX, 10TN, 10BX and 10BN in the ratio of 87:7:4:2.

7c. Reaction of N-oxide 1 with Methyl Acrylate.

A solution of 1(11mg, 0.62mmol) and methyl acrylate(0.2 ml, 2.1mmol) in acetonitrile(.2ml) was placed under 2.07KBar for 50 hours to complete the reaction. The solution was tested by HPLC every 5 hours until the peak corresponding to 1 disappeared. The NMR spectrum of the residue showed the methyl signals corresponding to 6TX, 6TN, 6BX and 6BN in the ratio of 46:19:24:11.

7d. Reaction of N-oxide 1 with Maleic Anhydride.

A solution of 1(17mg, 0.1mmol) and maleic anhydride(10mg, 0.1mmol) in acetonitrile(.35ml) was placed under the pressure of 1.38KBar for 6 hours. The solution did not give observable HPLC data because of the tailing of the maleic anhydride peak. The NMR spectrum of the residue showed methyl signals corresponding to 11TN and 11TX(or 11BX) in the ratio of 9:2. The methyl signals of two other cycloadducts were too feeble to be

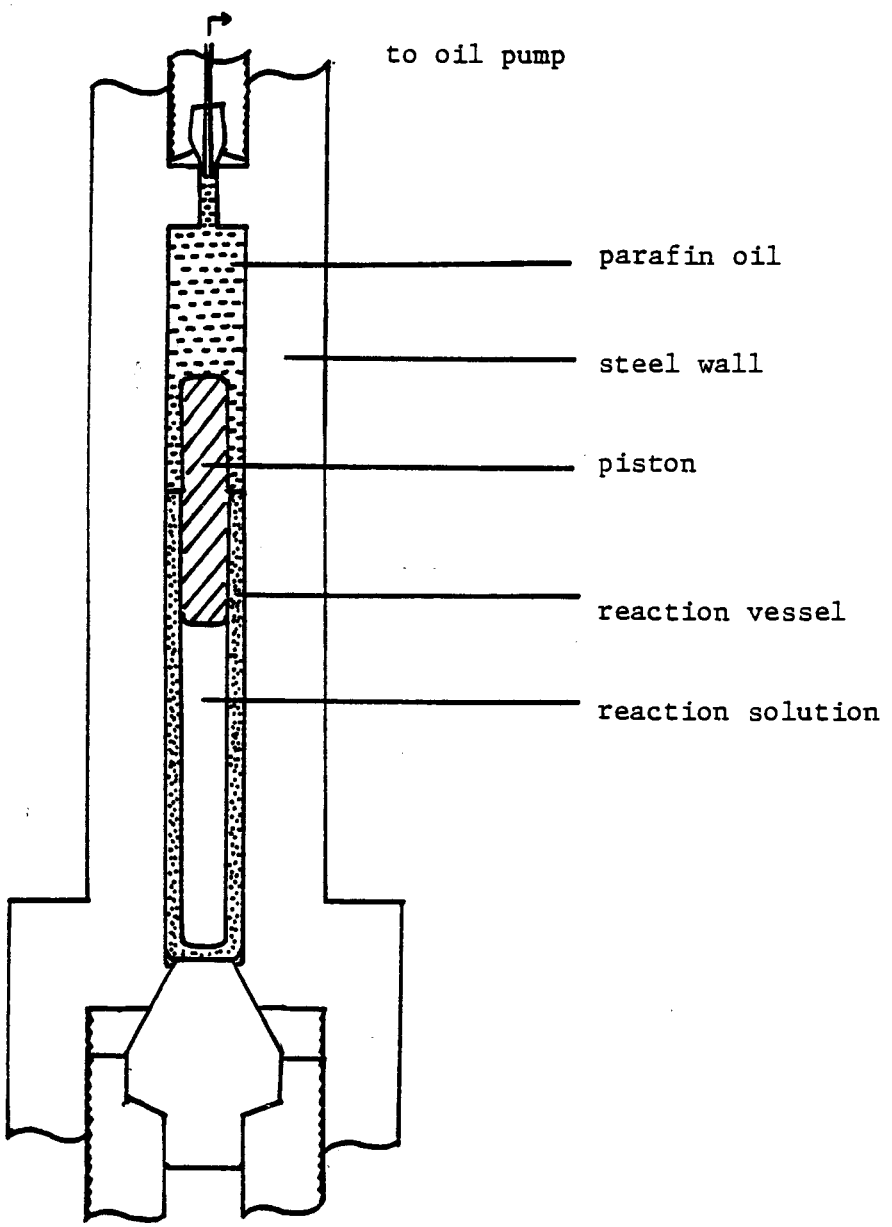

Figure 4-5. High pressure reaction apparatus.

integrated.

8. Formation Constants of the Ground State Complexes

Absorption spectra were measured with a Varian Cary 210 UV spectrophotometer at room temperature(22°C). The light path was 1mm for all of the experiments except for the measurement of the maleic anhydride complex for which 10mm cells were used. The ground state complexes were examined in the 250 to 500nm range. All the measurments were taken in acetonitrile. The data are given in the results section.

TABLE - 9 ^1H NMR PARAMETER

adducts	chemical shifts (splitting pattern) in ppm								coupling constants in Hz					
	H_a(dd)	H_b(dd)	H_c(dd)	H_d(dd)	H_e(dd)	H_f(dd)	CH_3(s)	OCH_3(s)	J_{ab}	J_{ac}	J_{bc}	J_{de}	J_{df}	J_{ef}
6TX	5.53	2.60	2.18	2.51	2.73	4.99	1.53	3.80	7.0	10.0	13.0	12.5	8.0	8.0
6TN	5.51	2.72	2.14	2.46	2.83	4.80	1.46	3.80	7.5	9.5	12.5	13.5	9.5	4.5
6BX	5.48	2.30	2.53	2.38	2.70	4.96	1.47	3.80	9.9	8.8	13.2	12.1	7.7	8.8
6BN[a]	2.36-2.63(3H), 2.73(dd,1H), 4.83(dd,1H) 5.25(dd,1H)						1.43							
7TX	5.59	2.74	2.29				1.63		6.5	10.5	12.5			
7TN[b]	5.65	2.62	2.13	2.60	2.43	5.22	1.58		6.5	10.0	12.5	12.5	6.5	10.0
8TX	5.50	2.60	2.18	2.63	2.83	5.13	1.63		7.5	9.8	13.5	13.5	6.0	8.3
8TN[c]	5.47	2.55	2.25	2.50	2.82	5.09	1.54		7.5	9.5	12.5	13.0	9.0	5.5
8BX[c]	2.22(dd,1H), 2.57(dd,1H), 2.75(dd,1H), 2.88(dd,1H), 5.00(dd,1H), 5.71(dd,1h).						1.52							
8BN[c]	2.60(dd,1H), 2.70-2.87(dd,3H), 5.03(dd,1H) 5.32(dd,1H).						1.46							

adducts	chemical shifts (splitting pattern) in ppm								coupling constants in Hz			
	H_a(dd)	H_b(dd)	H_c(dd)	H_d(d)	H_e(d)	CH_3(s)	OCH_3(s)		J_{ab}	J_{ac}	J_{bc}	J_{de}
9TX	5.70	2.66	1.95	3.73	5.20	1.62	3.81	3.82	8.5	8.0	13.0	7.5
9TN	5.42	3.07	2.20	3.98	5.33	1.33	3.81	3.82	7.0	8.0	13.0	6.0
9BN[d]	5.18	2.69	2.56	3.90	5.40	1.33	3.82	3.83	8.5	7.7	13.0	7.5
10TX	5.66	3.06	2.25	3.71	5.27	1.69			7.5	9.0	13.5	5.5
10TN[e]	5.68	2.90	2.33	3.93	5.12	1.67			8.0	9.0	13.5	6.0
10BX[f]	5.63	2.55	2.64	3.72	5.20	1.65			10.0	7.0	13.0	5.0
10BN[e]	5.40	2.53	2.71	3.88	5.18	1.63			8.0	8.5	13.0	6.0
11TN[g]	4.95	3.54	2.28	3.90	5.82	1.49			9.5	7.0	14.0	8.5
11BM[g]	5.77	3.13	1.87	3.93	4,74	1.57			9.0	8.0	13.0	9.0
12TX	5.50	2.80	2.26	3.82	5.22	1.48	3.77	3.84	7.0	9.0	13.0	8.0
12BX[h]	5.33	2.42	2.46	3.78	5.23	1.43	3.73	3.80	8.5	7.5	12.5	8.5

a. contaminated with 6TN in a ratio of 6BN/6TN = 2.3/1

b. 7TN =7BX.

c. tentatively assigned

d. contaminated with 9TX.

e. mixture of 10TX, 10TN, and 10BN in a ratio of 4:21:4.

f. mixture of 10TX, 10TN, 10BX and 10BN in a ratio of 3:4:32:1.

g. mixture of 11TN and 11BN in a ratio of 17:3.

h. mixture of 12TX and 12BX in a ratio of 3:1.

TABLE - 10 ^{13}C NMR PARAMETER

All spectra were taken in $CDCl_3$ except for adducts 11 which were taken in acetone-d_6.

adducts	Chemicial shifts (ppm)
6TX	170.74(C=O); 138.85, 128.61, 128.26, 126.42(Ph); 83.38, 77.31(C3&C7); 78.10(C5) 52.52(OCH_3); 48.36,43.89(C4&C6); 25.10(CH_3).
6BX	170(C=O); 139.98, 128.54, 127.94, 126.41(Ph); 83.87, 75.10(C3&C7); 77.81(C5) 52.51(OCH_3 : 46.59, 41.80(C4 &C6); 22.38(CH_3).
6TN[a]	128.55, 128.00, 126.29(Ph); 81.30(C3); 78.00(C5); 52.57(OCH_3); 47.59, 41.51(C4 & C6); 24.85(CH_3).
7TX	139.26, 128.58,.128.18,126.44(Ph); 83.42(C3 & C7); 78.97(C5); 49.72(C4 & C6); 26.03(CH_3).
7TN[b]	128.55, 127.98, 126.56, 126.28(Ph); 81.65, 79.38(C3 & C7); 78.40(C5); 49.00, 48.38 (C4 & C6); 24.92(OCH_3).
8TX	138.17, 128.74, 128.54, 126.37(Ph); 117.30(CN); 83.53, 64.76(C3 & C7); 78.14(C5); 48.19, 45.41(C4 & C6); 25.22(CH_3).
8TN[c]	128.69, 128.23, 126.27, 139.36(ph); 117.72(CN); 78.08(C5); 84.50, 63.72(C3 & C7); 46.01, 43.52(C4 & C6); 22.30(CH_3).
8BX[c]	138.68, 128.76, 128.26, 126.39(Ph);118.24(CN); 81.76, 65.81(C 3 &C7); 78.63(C5); 46.25, 43.91(C4 & C6); 22.89(CH_3).
8BN[c]	138.26, 128.70, 128.44, 126.48(Ph); 118.05(CN); 83.50, 65.51(C3 & C7); 78.49(C5); 47.00, 44.84(C4 & C6); 25.08(CH_3).

adducts	Chemical shifts (ppm)
9TX	170.18, 169.71(C=O); 138.52, 128.68, 128.32, 126.42(Ph); 85.10, 76.15(C3&C7); 79.94(C5); 57.60, 42.84(C4 & C6); 52.82, 52.75(OCH_3); 25.32(CH_3).
9BN[d]	170.45,170.01(C=O); 139.43, 128.01, 126.03(Ph); 82.24, 77.41(C3 & C7); 80.40 (C5); 57.14, 52.73(OCH_3); 45.84(C4orC6); 18.79(CH_3).
9TN	128.60, 127.92, 125.81(Ph); 81.38(C3orC7); 78.44(C5); 55.82, 47.33(C4&C6); 52.91, 52.59(OCH_3); 19.21(CH_3).
10TX	128.91, 128.89, 126.20(Ph); 114.86, 114.63(CN); 84.72,66.70(C3 & C7); 46.99, 44.75 (C4 & C6); 25.19(CH_3); 80.61(C5).
10TN[e]	137.91, 128.93, 128.83,126.16(Ph); 114.87, 114.14(CN); 82.46, 67.90(C3 & C7); 77.21(C5); 46.53, 46.30(C4 & C6); 22.17(CH_3).
11TN[g]	171.02(C=O); 144.11, 129.41, 128.48, 126.28(Ph); 84.12, 83.85(C3 & C7); 77.39 (C5); 54.29, 42.50(C4 & C6); 23.37(CH_3).
12TX	168.94, 168.85(C=O); 138.94, 128.69, 128.33, 126.26(Ph); 81.85, 79.26(C3 & C7); 77.20(C5); 58.00, 49.05(C4 & C6), 52.53, 52.32(OCH_3); 21.28(CH_3).
12BX[h]	165.59(C=O); 129.71, 128.09, 126.07(Ph); 80.23,(C3orC7); 57.29(C6); 52.25, 52.10 (OCH_3); 47.14(C4orC6); 19.48(CH_3); 79.85(C3orC7).

*The footnotes a,b,c,d,e,f,g,h are the same as in TABLE - 1.

TABLE - 11 IR ABSORPTIONS

adducts	solvent	absorption (cm^{-1})
6TN	I	2960 (m,b) , 1735 (s) , 1450 (w) , 1350 (w,b) , 1180 (w) , 1005 (w) , 830 (w,b) , 780 (w,b) .
6BX	I	2970 (m,b) , 1755 (s) , 1740 (s) , 1610 (m) , 1500 (w) , 1455 (w,b) , 1390 (w,b) , 1295 (w,b) , 1215 (m) ,1190 (w) , 1021 (w) , 840 (w) ,
6TX	I	2960 (m,b) , 1745 (s) , 1735 (s) , 1495 (w) , 1450 (m,b) , 1375 (w) , 1290 (m) , 1215 (s) , 1180 (m) , 1015 (m) , 965 (w) , 925 (w) , 815 (m) , 785 (w) .
7TX	I	3040 (m) , 3000 (m,b) , 1610 (m) , 1500 (m) , 1455 (s) , 1380 (m) , 1330 (m,b) , 1080 (w) , 1035 (m) , 1005 (m) , 955 (m) , 920 (m) , 860 (s) , 785 (m) .
7TN[b]	I	3040 (w) , 2980 (w,b) , 1610 (s) , 1500 (m) , 1460 (w) , 1385 (w) , 1340 (w) , 1055 (w) , 1040 (w) , 1000 (w) , 970 (w) , 930 (m) , 875 (s) , 835 (s) .
8TN[c,i]	I	3080 (s,b) , 2260 (w) , 1605 (w) , 1500 (m) , 1455 (s) , 1385 (m) , 1315 (m) , 1295 (m) , 1230 (m) , 1140 (w) , 1075 (w) , 1035 (m) , 1000 (m) , 975 (m) , 925 (m,b) , 850 (m,b) , 810 (m) , 795 (m) , 760 (s) , 705 (s) .
8TX	I	2960 (s,b) , 2260 (w) , 1500 (w) , 1460 (s) , 1380 (m) , 1315 (m) , 1290 (m) , 1230 (w) , 1045 (m,b) , 960 (m,b) , 880 (m) , 845 (w) , 814 (w) , 765 (s) , 705 (s) .
8BN[c,j]	I	3090 (m) , 2990 (s,b) , 2270 (w) , 1630 (w) , 1520 (m) , 1480 (s) , 1410 (m) , 1350 (m,b) , 1320 (m,b) , 1255 (m) , 1170 (w) , 1065 (m) , 1050 (m,b) , 950 (m,b) , 875 (m) , 815 (m) , 775 (s) , 730 (s) .
9TX	II	3040 (w) , 2940 (s,b) , 2870 (s) , 1745 (s) , 1730 (s) , 1455 (s,b) , 1380 (m) , 1350 (m) , 1310 (w) , 1285 (m) , 1250 (m) , 1230 (m) , 1210 (s) , 1180 (m) , 1020 (m) , 1000 (w) , 970 (m) , 915 (w) , 830 (w) , 800 (m) , 765 (m) , 745 (m) , 705 (m) .

adducts	solvent	absorptions (cm^{-1})
9TN	II	3040 (w), 2970 (s,b), 2860 (s), 1750 (s), 1740 (s) 1465 (s,b), 1440 (m), 1380 (m), 1340 (w), 1310 (w) 1270 (s,b), 1206 (s), 1185 (m), 1155 (w), 1025 (m) 1005 (m), 965 (m), 940 (w), 840 (w), 790 (w), 750 (m), 710 (m).
10TX	II	3080 (w), 2990 (s,b), 2880 (w), 1520 (w), 1480 (s) 1400 (m), 1375 (w), 1330 (m), 1315 (w), 1305 (w), 1260 (w), 1235 (w), 1205 (w), 1160 (w), 1070 (w), 1040 (s), 985 (m), 950 (m), 930 (w), 835 (m), 795 (s), 775 (m), 765 (w), 725 (s), 710 (m).
10BX[f]	III	3060 (w), 3035 (w), 2960 (s), 2934 (s), 2252 (w), 2854 (m), 1722 (s), 1556 (w), 1494 (m), 1456 (s) 1387 (m), 1348 (w), 1325 (w), 1288 (s), 1211 (w), 1184 (m), 1144 (w), 1074 (m), 1028 (s), 999 (m), 960 (m), 924 (m), 889 (w), 829 (w), 804 (w), 760 (s), 700 (s).
10TN[e]	III	3060 (w), 3035 (w), 2959 (s), 2928 (s), 2252 (w), 2854 (m), 1496 (m), 1454 (s), 1720 (m), 1554 (m), 1385 (m), 1288 (m), 1230 (w), 1149 (w), 1076 (w), 1026 (m), 987 (m), 968 (m), 910 (m), 845 (m), 806 (m), 760 (s), 702 (s).
11TN[g]	II	3000 (s,b), 1870 (w), 1785 (s), 1730 (m,b), 1460 (s), 1380 (m), 1230 (m), 1080 (w), 985 (w), 950 (m), 915 (m), 845 (w), 820 (w), 800 (w), 770 (m), 720 (w), 700 (m).
11BN[g]	II	3000 (s,b), 1875 (w), 1790 (s), 1465 (s), 1380 (m), 1345 (w), 1275 (w), 1265 (w), 1230 (m), 1090 (w), 995 (w), 920 (m), 850 (w), 820 (w), 805 (w), 775 (m) 730 (w), 715 (m).
12TX	II	3070 (w), 3040 (w), 3020 (w), 2960 (s), 2930 (s),

		2860(s), 1750(s,b), 1725(s), 1650(w), 1500(w), 1460(s), 1440(s), 1385(s), 1370(s), 1360(m), 1300(s), 1285(m), 1255(s), 1225(s), 1205(s), 1175(s), 1150(m), 1115(w), 1095(w), 1040(m), 1030(w), 1020(m), 1010(m), 985(w), 965(w), 920(w), 910(w), 865(w), 830(w), 810(m), 770(s) 750(w), 710(s).
12BX[h]	II	same as 12TX

I : CH_2Cl_2

II : nujol

III : neat

s: strong absorption, m: medium absorption, w: weak absorption.

b: absorption peak is broad.

The footnotes a, b, c, d, e, f, g and h are the same as in TABLE - 1.

i: mixture of 8TN and 8TX.

j: mixture of two 8 isomers which could be 8BX and 8BN.

TABLE - 12 UV ABSORPTIONS

adducts	absorption peak in nm
6TN	268(s), 264, 259(m), 252, 246(s), 242(s)
6BX	268(s), 265, 259(m), 253, 247(s)
6TX	268(s), 264, 259(m), 252, 247, 242(s)
7TX	267(s), 264, 258(m), 252, 247, 241(s)
7TN[b]	266(s), 263, 257(m), 251, 245
8TX	268, 264, 258(m), 252, 248(s), 242
9TN	269(s), 265(s), 259, 253(m)
9TX	273(s), 268(s), 264(s), 258(s)
10TX	268, 263, 257(m), 252, 247(s)
10TN[e]	282(s), 268, 262, 258(m), 252
10BX[f]	282, 269(s), 264, 257, 251(s)
11TN[g]	268(s), 264(s), 261(s), 257, 251(s)

*all the spectra were taken in CH_2Cl_2.

m: maxium; s: shoulder

The footnotes b, e, f and g are the same as in TABLE - 1.

Table-13. Mass Spectra Data.

Adducts m/e	6TX %	6BX %	6TN %	7TX %	7TN[b] %	8TN[c] %	8TX %
41	15	39	30	36	35	7	16
42	12						
43	8	36	35	11	17	9	16
51	28	24	26	16	17		
55	18	30	24	5			25
56	2	13	7				
57	2	12	5				27
65	16	16	15				
67	12	19	15			11	21
69		22	9				34
70						12	
71		12	6	21	22		28
72		28					
73		6	2				
77	100	64	100	50	50	21	36
78	45	28	46	18	20		15
79	12	12	23	11	12		15
81		10	5				21
82		10					10
83		12					28
84							11
85		14					23
91	80	90	43	48	51	32	33
94						11	11
95	15	25	23				19
97		19					28
99	17	56	7				11
100		34					
103	34	22	26	14	16		10
104	53	100	32	20	21	100	100
105	74	57	86	47	58	33	41
107				11	11	55	50
109							13
111							17
113		2	26				
115	37	21	22	12	13		10
127	31	32	15				
128	31	17	19		10		
129	53	33	34	18	24	14	18
130	25	14	15	49	43		

adducts m/e	6TX %	6BX %	6TN %	7TX %	7TN[b] %	8TN[c] %	8TX %
131	57	46	20	19	18		
143	13	8	7				
145	38	23	15	100	100		10
149							18
153	73	2	2				
155	10	33	43				
173	25	12	6				
183	21	9	12				
215	60	20	10				

Adducts m/e	9TX %	9TN %	10TX %	e 10TN %	f 10BX %	h 12BX %	12TX %	g 11TN %
41	10	23	9	25	13	16	13	12
42		10						
43	9	21	8	27	13	19	21	10
51		11	13			13	13	11
55	11	21		36	14	12	11	14
56		22		11				
57		40		48	25			
59	23	32	11			40	42	
60				20				
63		13						
65						11	11	
67	13	17		20		12	12	11
68			15					
69	19	39	13	77	17	19	16	25
70				31	17			
71	11	20		52	25			
73		12		44				
77	41	52	40	25	17	52	52	37
78	18	30	20	13		26	27	15
79			24	24	10			12
81		12		43				12
82		11		21		11	11	
83	11	16		44	15			23
84				29				
85	17	24		36		18	18	
86		25						
87				12				
91	39	58	32	17	11	56	58	92
92			15					
93				12				
95		11		21				18
97				33				
98	13	14		18		25	25	
99	17	17		15		15	16	
101	14	24				18	16	
103	11	16	15			20	20	11
104	100	100	100	32	25	100	100	100
105	44	42	42	31	19	54	50	45
107			48	31	16			17
109				13				
111				18				25
112				12	10			

adducts m/e	9TX %	9TN %	10TX %	e 10TN %	f 10BX %	h 12BX %	12TX %	g 11TN %
113	33	24		18		71	73	
115	11	16	15	14		19	19	
117						14	14	
121	12	18		11		21	20	
125	27	29				24	24	
126	34	23						
127	14	16				29	30	
128	20	32	24			39	41	20
129	44	61	28	27	11	66	68	42
130		11				21	22	
131	13	17				27	27	
137				10				
140						11	12	
143	11	15		40	13	22	22	
145						32	33	
149	18			100	100			
153		12				33	34	
155	29	21				21	20	
157	14	12				43	44	
158	15	11				30	30	
161						15	14	
167				31	35			
170			75	17	14			
171	39	65	10			72	74	23
172		11				14	14	
173								45
185						21	22	
199	21	21				15	15	11
203	15	20				48	48	
214						15	15	
230	26	20				35	37	
240	11	13				23	24	
262						15	16	
279				12	10			

Those under 10% abundance are not reported.

The footnotes b, c, e, f, g, and h are the same as in Table-1.

TABLE - 14 NOE RESULTS.

Table -14. 1.

adducts	proton(s) irradiated	percentage enhancement Ha	Hb	Hc	Hd	He	Hf	CH_3
6TX	CH_3			2.7	2.1			
	H_a		5.8	1.4		1.7	8.6	
	H_f	5.3	2.1		2.1	6.4		
6BX	CH_3	2.7		2.7	2.7			
	H_a		1.6	6.5				
	H_f		w		1.6	4.5		
6TN	H_a		5.9	w		3.9		
	H_c	w	s					w
	H_d					s	s	w
	H_f				6.3			

Table -14. 2.

adducts	proton(s) irradiated	percentage enhancement Ha	Hb	Hc	Hd	He	Hf	Ph
7TX	CH_3			3.4				
	H_a		7.6					
	H_b	10.3		30.9				
	H_c		24.1					w
7TN	CH_3			1.2	1.3		1.5	
	H_a		3.0			3.7		14.0
	H_f				7.5			12.6

Table -14. 3.

adducts	proton(s) irradiated	percentage enhancement					
		Ha	Hb	Hc	Hd	He	Hf
8TX	CH_3			3.2	7.2		
	H_a		5.6	w		w	7.4
	H_f	5.0	w		1.3	5.6	

Table -14. 4.

adducts	proton(s) irradiated	percentage enhancement				
		Ha	Hb	Hc	Hd	He
9TN	CH_3			3.8		4.5
	H_b	m		s	8.3	
	H_c		19.3			
	H_d	13.9	m			8.2
9BN	CH_3			4.8		4.8
	H_a		w	5.4		
	H_d		8.7			15.2
	H_e				s	
9TX	CH_3			4.2	5.8	
	H_a		7.1	2.0		7.1
	H_b	13.3		31.4		6.7
	H_c	4.5	30.9			
	H_e	6.2	4.6			

Table -14. 5.

adducts	proton(s) irradiated	percentage enhancement Ha	Hb	Hc	Hd	He
10TX	CH_3			2.3	1.5	
	H_a		5.7	1.4		4.8
	H_b	12.0		28.0		4.1
	H_c	5.2	26.0			
	H_d					12.0
	H_e	6.7			4.5	
10TN	CH_3			3.9	0.5	1.4
	H_a		5.1	1.7	6.8	
	H_b	11.7		23.7	11.0	
	H_c	6.3	23.8			
	H_e				3.8	
10BN	CH_3	2.2		4.3		1.9
	H_a		1.3	3.1		
	H_b	4.9		7.4	9.9	
	H_c	16.3	20.9			
	H_d		8.3			2.8
10BX	CH_3	3.4		3.8	6.8	
	H_a		1.4	9.3		

Table - 14.6

adducts	proton(s) irradiated	H a	H b	H c	H d	H e	CH_3	Ph
12TX	CH_3			5.0				
	H_a		4.8	2.0	5.6	8.9		11.3
	H_b	10.6		27.7	14.9	3.2		
	H_c	0.9	21.8				3.6	5.7
	H_e	2.3	1.8		12.5			
12BX	CH_3	5.0		5.0				
	H_b	2.7		16.0	10.7	5.3		
	Hc	11.0	18.6					

Table - 14.7

adducts	proton(s) irradiated	%enhancement H_a	H_b	H_c	H_d	H_e
11TN	CH_3			2.6	5.8	0.6
	H_a		6.0	2.4		
	H_b	15.7		22.6		
	H_c	8.8	33.3			
	H_d					14.1
	H_e				8.0	
11BN	CH_3			3.9	6.7	
	H_c	6.1	16.3			
	H_d					4.3
	H_e				6.7	

w: weak enhancement without integration.

m: medium enhancement without integration.

s: strong enhancement without integration.

TABLE - 15 ELEMENTAL ANALYSES

adducts	C %	H %	N %
6TX	63.88	6.60	5.40
6TN	63.62	6.42	5.50
calculated	63.87	6.51	5.32
7TX	76.92	6.73	5.17
7TN	77.00	6.39	4.92
calculated	76.84	6.81	4.98
9TN	60.09	6.06	4.38
9TX	59.98	5.98	4.25
calculated	59.81	5.96	4.36
8TN[a]	68.09	6.21	11.90
8TX	68.04	6.01	12.26
8BX[b]	68.02	6.16	12.19
calculated	67.81	6.13	12.17
10TX	65.78	5.23	16.75
calculated	65.87	5.13	16.46
11TN	61.01	4.59	5.30
calculated	61.09	4.76	5.09
12TX	59.96	6.04	4.30
12BX[c]	59.61	5.93	4.43
calculated	59.81	5.96	4.36

a: mixture of 8TX and 8TN in the ratio of 4/3.
b: mixture of 8BX and 8BN in the ratio of 11/6.
c: mixture of 12TX and 12BX in the ratio of 3/1.

REFERENCES

1. R. Huisgen, Angew. Chem. Int. Ed. Engl., 2, 562 (1963).
2. R. Huisgen, Angew. Chem. Int. Ed. Engl., 2, 633 (1963).
3. W. Oppolzer, Angew. Chem. Int. Ed. Engl, 16, 10 (1977).
4. R. Huisgen, J. Org. Chem., 41, 403 (1976).
5. R. A. Firestone, J. Org. Chem., 33, 2285 (1967).
6. R. A. Firestone, Tetrahedron, 33, 3009 (1977).
7. R. Huisgen, J. Org. Chem., 33, 2291 (1968).
8. M. S. Haque, J. Chem. Educ., 61, 490 (1984).
9. B. M. Benjamin and C. J. Collins, J. Am. Chem. Soc., 95, 6145, (1973).
10. E. Eckell, R. Huisgen, R. Sustman, G. Wallbillich, D, Grashey, E. Spinlder, Chem. Ber., 100, 2192 (1967).
11. R. Hoffmann and R. B. Woodward, Angew. Chem. Int. Ed. Engl., 8, 781 (1969); ibid, 9, 817 (1969).
12. K. N. Houk, J. Am. Chem. Soc., 94, 8953 (1972).
13. A. R. Katritzky, A. J. Boulton, "Advances in Heterocyclic Chemistry", Vol.21, Academic Press, N .Y. 1977, p. 208.
14. R. Grashey, R. Huisgen, and L. Leitermann, Tetrahedron Lett, 9 (1960).
15. C. W. Brown and M. A. T. Rogers, British Paten., 850, 485 [CA, 55, 6498 (1961)].
16. V. A. Tartakovskii, I. E. Chlenov, G. W. Lagodzinskaya, S. S. Novikov, Chem. Abstr.,62,14646(1965).
17. V. A. Tartakovskii, A. A. Onishchenko, and S. S. Novikov, Zh. Org. Khim., 3, 588 (1967)[CA 32625g (1967)].

18. S. Patai, "The Chemistry of the Nitro and Nitroso Groups" Part I, N. Y., 1969, p.454.

19. R. Gree, F. Tonnard, R. Carrie, Tetrahedron Lett., 453 (1973); 2987 (1972).

20. R. Gree, R. Carrie, Tetrahedron, 32, 683 (1976).

21. S. L. Ginzburg ,M. G. Neigauz, L. A. Novakovskaya, S. S. Novikov, V. A. Tartakovskii, I. E. Chlenov, Z. A. Akopyan, A. I. Guser, Yu. T. Struchkov, Zh. Strukt, Khim., 10 (5), 877-881 [CA 72, 32764(1970)].

22. A. I. Ivanov, V.I. Slovetskii, V. A. Tartakovskii, S. Novikov, Chem. Abstr., 65, 4848 (1966); 65, 3852 (1966) 64, 2079 (1966).

23. N. A. Lebel and J. J. Whang, J. Am. Chem. Soc., 89, 3076 (1976).

24. V. A. Tartakovskii, Z. Ya. Lapshina, I. A. Savost'yanova, S. S. Novikov, Zh. Org. Khim., 4, 236 (1968) [CA 68, 95734 (1969)]. V. A. Tartalovskii, I. E. Chenov Morozora, and S. S. Novikov, Izv. Akad. SSSR, Khim., 370 (1966)[CA 64, 17567(1966)].

25. V.A.Tartakovskii, S. S. Smagin, I. E. Chlenov, S. S. Novikov, SSSR, Ser. Khim., 552 (1965)[CA 63, 594 (1965)].

26. V. A. Tartakovskii, A. A. Onishchenko, Zh. Org. Khim., 3, 1079 (1967).

27. V. A. Tartakovskii, A. A. Onishchenko, V. A. Smirnyadin, and S. S. Novikov, Zh. Org.

Khim., 2, 2225 (1966).

28. Y. L. Chow, B. H. Bakker, Synthesis, 8, 648 (1982).

29. M. Clagett, A. Gooch, P. Graham, N. Holy, B. Mains, and J. Strunk, J. Org. Chem., 41, 4033 (1976).

30. J. H. Noggle, R. H. Schirmer "The Nuclear Overhauser Effect", Academic Press, N. Y., 1977.

31. J. K. Samders, J. W. Easter, "Determination of Orgainc Structures by Physical Methods"., Vol. 6, Academic Press, N. Y., 1976.

32. T. Schimizu, Y. Hayashi, and K. Teramura, J. Org. Chem., 48, 3053 (1983).

33. T. Nakono, C. Rivas, C.Perez, and K. Tori, J. Chem. Soc., Perkin I, 2322 (1973).

34. A. Lablache-Combier, M.-L. Villaume, Tetrahedron Lett., 49, 4959 (1976).

35. F. A. L. Anet, A. J. R. Bourn, P. Carter, and S. Winstein, J. Am. Chem. Soc., 87, 5249 (1965).

36. R. S. Mulliken, J. Am. Chem. Soc., 72, 600 (1950); 72, 4493 (1950).

37. J. B. Birks, "Photophysics of Aromatic Molecules", Wiley, N. Y., 1970, p.40.

38. S. Mukherjee, S. K. DE, and S. R. Palit, Indian J. Chem., 11, 547 (1973).

39. A. Padwa, L. Fisera, K. F. Koehlder, A. Rodriguez, and S. K. Wang, J. Org. Chem., 49, 279 (1984).

40. R. Gree, F. Tonnard, R. Carrie, Tetrahedron, 32, 675

(1976).

41. P. Ashburn, R. M. Coates, J. Org. Chem., 49, 3127 (1984).
42. V. M. Shitkin, V. A. Korenevskii, V. G. Osipov, M. V. Kashtina, S. L. Ioffe, I. E. Chlenov, V. A. Tartakovskii, Zh. Org. Khim., 8, 864, (1972).
43. R. Gree, F. Tonnard, R. Carrie, Bull. Soc. Chim., 5-6, 1325 (1975).
44. K. N. Houk, J. Simus, R. E. Duke., Jr., R. W. Strozier and J. K. George, J. Am. Chem. Soc., 95, 7287 (1973).
45. K. N. Houk, J. Sims, C. R. Watts, L. J. Luskus, J. Am. Chem. Soc., 95, 7301(1973).
46. W. C. Herdon, Chem. Rev., 72, 157 (1972).
47. R. Sustman, Pure Appl. Chem., 40, 569 (1974).
48. R. Gree, F. Tonnard, R. Carrie, Tetrahedron, 32, 675 (1976).
49. J. Bastide, N. E. Ghandour and O. Henri-Rousseau, Bull. Soc. Chim., 2290 and 1194 (1973); 1037 (1974).
50. I. Fleming, "Frontier Orbitals and Organic Chemical Reactions", Wiley, N. Y., 1976, p.110, 132.
51. R. Hoffmann and R. B. Woodward, J. Am. Chem. Soc., 87, 4388 (1975).
52. R. Gree, R. Carrie, Bull. Soc. Chim(Fr), 1319 (1975).
53. R. Gree, F. Tonnard, R. Carrie, Tetrahedron Lett., 2, 135 (1974).
54. K. N. Houk, Acc. Chem., Res., 8, 361 (1975).
55. N. S. Isaacs and E. Rannala, J. Chem. Soc., Perkin II, 1955 (1975).

56. K. Matsumoto, Y. Ikemi-Kono, J. Chem. Soc. Comm., 543 (1978).

57. J. Jurczak and M. Tkacz, J. Org. Chem., 44, 3347 (1979).

58. C. M. Dicken and P. Deshong, J. Org. Chem., 47, 2047 (1982).

59. S. Mukherjee, S. R. Palit, J. Phys. Chem., 74, 1389 (1970).

60. M. Sasaki, H. Tsuzuki, J. Osugi, J. Chem. Soc., Perkin II, 1596 (1980)